LIMNOLOGY
and
OCEANOGRAPHY

ASLO

*Limnol. Oceanogr.* 00, 2019, 1–19

doi: 10.1002/lno.11236

# Dynamics of benthic metabolism, $O_2$, and $pCO_2$ in a temperate seagrass meadow

**Peter Berg**,[1]* **Marie Lise Delgard**,[1] **Pierre Polsenaere**,[2] **Karen J. McGlathery**,[1] **Scott C. Doney**,[1] **Amelie C. Berger**[1]

[1]Department of Environmental Sciences, University of Virginia, Charlottesville, Virginia
[2]Resources and Environment Laboratory, IFREMER, L'Houmeau, France

## *Abstract*

Seagrass meadows play an important role in "blue carbon" sequestration and storage, but their dynamic metabolism is not fully understood. In a dense *Zostera marina* meadow, we measured benthic $O_2$ fluxes by aquatic eddy covariance, water column concentrations of $O_2$, and partial pressures of $CO_2$ ($pCO_2$) over 21 full days during peak growing season in April and June. Seagrass metabolism, derived from the $O_2$ flux, varied markedly between the 2 months as biomass accumulated and water temperature increased from 16°C to 28°C, triggering a twofold increase in respiration and a trophic shift of the seagrass meadow from being a carbon sink to a carbon source. Seagrass metabolism was the major driver of diurnal fluctuations in water column $O_2$ concentration and $pCO_2$, ranging from 173 to 377 $\mu$mol $L^{-1}$ and 193 to 859 ppmv, respectively. This 4.5-fold variation in $pCO_2$ was observed despite buffering by the carbonate system. Hysteresis in diurnal water column $pCO_2$ vs. $O_2$ concentration was attributed to storage of $O_2$ and $CO_2$ in seagrass tissue, air–water exchange of $O_2$ and $CO_2$, and $CO_2$ storage in surface sediment. There was a ~ 1:1 mol-to-mol stoichiometric relationship between diurnal fluctuations in concentrations of $O_2$ and dissolved inorganic carbon. Our measurements showed no stimulation of photosynthesis at high $CO_2$ and low $O_2$ concentrations, even though $CO_2$ reached levels used in IPCC ocean acidification scenarios. This field study does not support the notion that seagrass meadows may be "winners" in future oceans with elevated $CO_2$ concentrations and more frequent temperature extremes.

Seagrass meadows are metabolic hotspots in shallow coastal waters. It has long been known that their high rates of primary production and respiration accelerate nutrient cycling and support diverse consumer communities (Costanza et al. 1997; Beck et al. 2001; McGlathery et al. 2007). As such, seagrass meadows are valued for their role as a nutrient filter that improves water quality and as a nursery ground for many commercially important fisheries. More recently, seagrass meadows, and other coastal vegetated systems such as salt marshes and mangroves, have been recognized for their importance in "blue carbon" sequestration and storage (Duarte et al. 2005; Mcleod et al. 2011; Greiner et al. 2013). This has spurred substantial international research to understand the role of coastal vegetated habitats in carbon retention on regional and global scales (Johannessen and Macdonald 2016; Macreadie et al. 2018; Oreska et al. 2018). This framework is currently used to develop strategies to mitigate and adapt to climate change through conservation and restoration of coastal vegetation (Murray et al. 2011; Hejnowicz et al. 2015).

$O_2$ and $CO_2$ concentrations in the water column of seagrass meadows are generally strongly correlated, despite the buffering capacity of the carbonate system, and are driven primarily by plant metabolism (Semesi et al. 2009; Hendriks et al. 2014; Pacella et al. 2018). For *Zostera marina*, discrete (Buapet et al. 2013) and continuous (Ruesink et al. 2015) measurements have shown that the most significant variability in $O_2$ concentrations and partial pressures of $CO_2$ ($pCO_2$) in the water column of seagrass meadows occur at diel and tidal time scales overlaid with seasonal variations (Duarte et al. 2013*a*; Waldbusser and Salisbury 2014). It has been suggested that in some seagrass systems, especially in the tropics, calcium carbonate ($CaCO_3$) precipitation and dissolution also can affect $CO_2$ concentrations and fluxes (Mazarrasa et al. 2015; Howard et al. 2018; Saderne et al. 2019). Calcium carbonate precipitation is a net source of $CO_2$ (depleting $CO_3^{2-}$ and reducing total alkalinity (TA) will increase $pCO_2$), whereas carbonate dissolution contributes to the $CO_2$ sink, at the time scales often used for estimating seagrass metabolism (Macreadie et al. 2017). However, there is a wide range of values reported in the literature (Mazarrasa et al. 2015;

*Correspondence: pb8n@virginia.edu

Saderne et al. 2019), and much uncertainty about the role inorganic carbon processing plays in carbon sequestration of blue carbon systems (Macreadie et al. 2017). A recent global assessment of inorganic carbon burial rates concluded that this burial is mainly supported by inputs from adjacent ecosystems such as salt marshes and mangrove forests (Saderne et al. 2019). In some seagrass ecosystems, $O_2$ and $CO_2$ concentrations may also be influenced by external inputs from rivers (Aufdenkampe et al. 2011; Ruesink et al. 2015), from coastal upwelling (Feely et al. 2008; Saderne et al. 2013), or from benthic systems adjacent to seagrass meadows (Wang and Cai 2004; Guo et al. 2009) or mangroves (Bouillon et al. 2007; Yates et al. 2007). This can result in supersaturation of both $O_2$ and $pCO_2$ simultaneously in the water column of seagrass meadows (Ruesink et al. 2015).

Two main climate-related drivers, temperature and ocean acidification, affect seagrass metabolism. However, there is some debate about whether, and where, seagrass meadows will be winners or losers in future oceans. It has long been known that temperatures exceeding tolerance thresholds of seagrass species result in localized dieback events (Moore and Jarvis 2008; Marba and Duarte 2010; Thomson et al. 2015), and recent studies have documented the potential impact of marine heat waves on seagrass sediment carbon stores (Arias-Ortiz et al. 2018). Loss of seagrass biomass and oxidation of sediment carbon can result in seagrass meadows shifting from a sink to a source of carbon. The effect of ocean acidification from increasing $CO_2$ concentrations is more equivocal. Laboratory studies with leaf fragments have typically shown a positive short-term (hours) response to $CO_2$ enrichment (Zimmerman et al. 1997; Borum et al. 2016). This is predicted based on $HCO_3^-$ use by seagrass species and the lower energetic costs of switching to direct $CO_2$ uptake (Koch et al. 2013). However, mesocosm incubations done with transplanted individual shoots have shown mixed results, with only some species showing increases in productivity with higher water column $CO_2$ concentrations (Palacios and Zimmerman 2007; Collier et al. 2018). Field studies taking advantage of natural gradients in $CO_2$ concentrations also have shown no consistent positive response to elevated $CO_2$ (Ruesink et al. 2015; Takahashi et al. 2015; Koopmans et al. 2018). These apparently conflicting findings highlight the importance of assessing seagrass responses in natural communities under in situ conditions that reflect the complex interacting factors of inorganic carbon sources, light, flow, and temperature (Koch et al. 2013; Pedersen et al. 2013; Takahashi et al. 2015).

This study explores the relationship between whole-system benthic metabolism and concurrent water column concentrations of $O_2$ and $pCO_2$ for a temperate *Z. marina* seagrass meadow. The work was done exclusively in situ and relied on state-of-the-art approaches. The site used is located on the coast of Virginia, U.S.A., and is part of the Virginia Coast Reserve Long-Term Ecological Research domain. It has been a designated area for landscape-scale seagrass restoration by seeding and general seagrass research for nearly two decades (e.g. Orth et al. 2006; McGlathery et al. 2012). In the present study, we quantified shifts in carbon source-sink relationships driven by changes in seagrass metabolism during a period when temperatures nearly doubled from spring to summer. We also used our in situ measurements to investigate whether naturally elevated $CO_2$ and reduced $O_2$ concentrations in the water column stimulated seagrass photosynthesis when light was not a limiting factor. Combined, our high-resolution in situ data provided new insights on temperate seagrass metabolism and its controls that may also be used to forecast climate impacts on these ecosystems.

A critical challenge to assessing whole-system seagrass metabolism has been limited by our ability to accurately quantify rates of production and respiration as well as their dynamics over multiple time scales (Hume et al. 2011; Rheuban et al. 2014*b*; Long et al. 2012). With conventional methods, including in situ chamber measurements and laboratory or mesocosm incubations of either vegetated sediment cores or individual plant segments, it is difficult, if not impossible, to mimic natural dynamic field conditions of water column concentrations, light, flow, and temperature (Pedersen et al. 2013). In this study, we relied on the aquatic eddy covariance technique (Berg et al. 2003*a*) that largely circumvents these challenges due to its noninvasive nature (Lorrai et al. 2010), high temporal resolution (Rheuban and Berg 2013), and its ability to integrate over a large benthic surface (Berg et al. 2007). The aquatic eddy covariance technique provides the best estimate of whole-system seagrass metabolism under true field conditions that can be produced today.

## Methods

### Study site

The study site is located in South Bay (37°15′43.6356″N, 75°48′54.547″W; Fig. 1) on the coast of Virginia, U.S.A., and has been a designated area for a landscape-scale seagrass restoration project initiated in the early 2000s (Orth et al. 2006, 2010; Orth and McGlathery 2012).

The study reported here is connected to a larger effort focused on understanding the state change that has occurred over the last two decades from bare sediment to seagrass dominance in the shallow coastal lagoons as part of the Virginia Coast Reserve Long-Term Ecological Research (VCR LTER) project (Hansen and Reidenbach 2012; McGlathery et al. 2012; Greiner et al. 2013; Reynolds et al. 2013; Carr et al. 2016; Oreska et al. 2017). Since 2007, an important component of this work has been aquatic eddy covariance measurements of benthic $O_2$ fluxes from which seagrass metabolism and its controls have been quantified (Hume et al. 2011; Rheuban et al. 2014*a*,*b*; Berg et al. 2017).

South Bay is a shallow coastal lagoon bound by tidal channels in between barrier islands and salt marshes. It has no riverine inputs as indicated by a near-constant salinity (Table 1), and it has high water quality due to low watershed nutrient

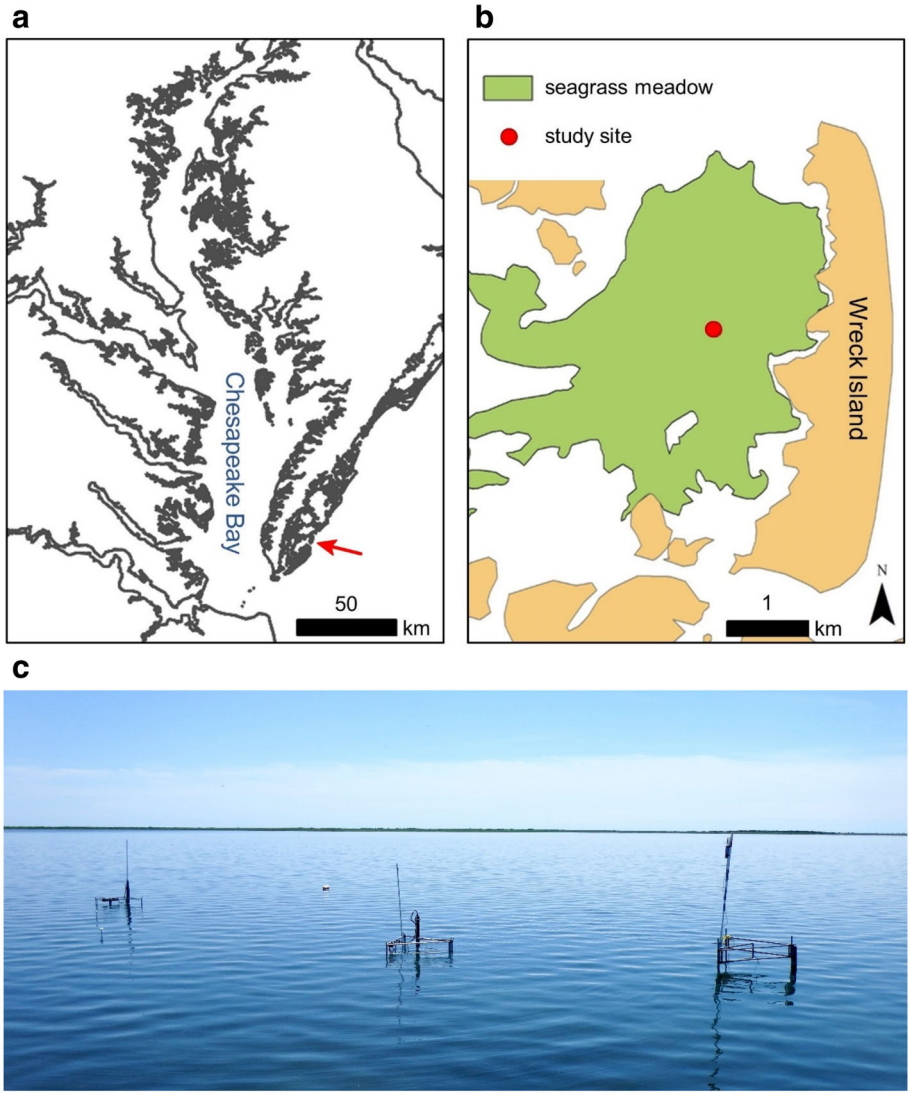


**Fig. 1.** (**a**) Location of the study site in South Bay on the Atlantic side of the Delmarva Peninsula, Virginia, U.S.A. (**b**) Aerial map of the ~ 7 $km^2$ large *Z. marina* meadow in South Bay behind Wreck Island with the study side located in its center. (**c**) Site picture taken at low tide of the two deployed aquatic eddy covariance systems (left), and a third frame (right) holding the $pCO_2$, pH, salinity, and turbidity sensors at canopy height.

inputs (McGlathery et al. 2012). The study site is located behind the ~ 5 km long Wreck Island and is protected from ocean swells while still allowing water exchange with the Atlantic Ocean (Fig. 1). Water depth at the site is 1.15 m at mean sea level with an average ~ 1 m tidal range (Table 1), and sediments consist primarily of siliciclastic sand and silt-size particles with low carbonate content (Wiberg et al. 2015). The site is located in the center of a dense *Z. marina* meadow (Fig. 1; Table 1) covering approximately 7 $km^2$ as of 2015.

### Aquatic eddy covariance measurements

Data were collected during 12 d in late April and early May 2015, and 14 d in late June 2015. For simplicity, we refer to these two sampling periods below as "April" and "June."

Benthic $O_2$ fluxes were measured with two aquatic eddy covariance systems (Berg et al. 2003*a*, 2017; Berg and Huettel 2008) deployed simultaneously less than 10 m apart (Fig. 1). The systems were lined up relative to the dominant tidal current direction so that they did not interfere with one another. This duplication ensured a good deployment success rate.

Each system consisted of an acoustic Doppler velocimeter (a Vector from Nortek-AS) coupled to a fast responding (90% response time $t_{90\%} < 0.4$ s) Clark-type $O_2$ microelectrode (Unisense), via a submersible pico-amplifier (McGinnis et al. 2011). The sensors were mounted on a light stainless steel frame designed to minimize disturbances of the natural flow (Berg and Huettel 2008). Data were recorded continuously at 32 Hz at a point at the average seagrass canopy height at slack tide, corresponding to 30 cm above the sediment surface. At this

**Table 1.** Means, minima, and maxima for hourly temperature, salinity, water depth, PAR, $O_2$ concentration, $pCO_2$, and pH, followed by shoot density, shoot length, and above and below ground biomass for the two sampling periods.

| | Apr | | | | Jun | | | |
|---|---|---|---|---|---|---|---|---|
| | **Mean** | **Min** | **Max** | ***n*** | **Mean** | **Min** | **Max** | ***n*** |
| Temperature (°C) | **16.0** | 12.5 | 21.4 | 208 | **27.6** | 24.0 | 30.9 | 299 |
| Salinity (ppt) | **31.8** | 31.4 | 32.4 | 207 | **31.9** | 30.3 | 32.9 | 297 |
| Turbidity (NTU) | **33** | 0 | 698 | 207 | **214** | 2 | 658 | 298 |
| Water depth (m) | **1.14** | 0.64 | 2.00 | 201 | **1.16** | 0.64 | 1.92 | 260 |
| PAR ($\mu$mol $m^{-2}$ $s^{-1}$) | **435** | 0 | 2280 | 214 | **342** | 0 | 2290 | 312 |
| $O_2$ ($\mu$mol $L^{-1}$) | **279** | 189 | 377 | 214 | **236** | 173 | 346 | 299 |
| $pCO_2$ (ppmv) | **425** | 193 | 731 | 207 | **490** | 256 | 859 | 297 |
| pH (0–14) | | N.A. | | | **8.09** | 7.80 | 8.26 | 136 |
| Shoot density ($m^{-2}$) | **316** | 256 | 384 | 8 | **230** | 192 | 288 | 8 |
| Shoot length (cm) | **23** | 20 | 29 | 5 | **34** | 24 | 42 | 6 |
| Aboveground biomass (g $core^{-1}$) | **0.63** | 0.06 | 1.01 | 5 | **0.92** | 0.09 | 1.80 | 6 |
| Belowground biomass (g $core^{-1}$) | **0.81** | 0.12 | 1.33 | 5 | **1.00** | 0.38 | 1.60 | 6 |

measuring height, $O_2$ fluxes originated from a relative large area (> 100 $m^2$; Berg et al. 2007) and thus were well integrated over the typical patchiness of the seagrass meadow (Rheuban and Berg 2013). To avoid damaging the microsensors at slack tide when seagrass leaves extend vertically, the canopy was cut in a 0.25 $m^2$ area directly below the sensors (Hume et al. 2011; Rheuban et al. 2014*b*). Continuous 48-h long deployments were performed in succession during each sampling period, separated by 2–3 h downtime while data were downloaded, batteries replaced, and the $O_2$ microelectrode checked, cleaned, or replaced as needed. For each deployment, care was taken to ensure that the instrument frames were as level as possible to minimize postprocessing rotations of the velocity field to correct for sensor tilt. Overall, a total of 21 full days of high-quality aquatic eddy covariance data were recorded for April and June, and from them, first eddy fluxes and then metabolic numbers were extracted as described below.

### $O_2$ measurements

Mean $O_2$ concentration and temperature were measured concurrently in the water column at canopy height (30 cm) once per minute using autonomous submersible $O_2$ optodes (miniDOT, PME). This stable (minimum drift) type of optode has a response time of approximately $t_{90\%}$ ~ 30 s, and was used to characterize the water column and to calibrate the $O_2$ microelectrodes used in the aquatic eddy covariance systems. The $O_2$ optodes were inspected or replaced after each ~ 48 h deployment. If the latter, the sensors were brought back to the lab and cleaned for any visible biofouling.

### $pCO_2$ measurements

Partial pressures of $CO_2$ ($pCO_2$) were similarly measured in the water column at canopy height using an autonomous $pCO_2$ underwater sensor well suited for long-term shallow-water applications (Mini-Pro $CO_2$ Pro; Oceanus System). It uses a tubular interface that combines three means of biofouling resistance, and it has an oil resistant semipermeable membrane that allows rapid diffusion of gas from the water to a non-dispersive infrared detector. The output is corrected for pressure and temperature variations. The measurement range is 0–2000 ppmv with a resolution of 1 ppmv, an absolute accuracy of 40 ppmv, and a response time ($t_{63\%}$) of ~ 3 min. Values of $pCO_2$ were recorded using a continuous mode with a sampling frequency of 0.5 Hz. The probe was calibrated by the manufacturer prior to the study, and the internal zeroing baseline correction ensured minimum drift. More information on the sensor is given by Schar et al. (2010), Wanninkhof et al. (2013), and Ge et al. (2014).

### pH measurements

Values of pH were measured during three 48-h deployments in the water column just above the canopy next to the $pCO_2$ sensor with two digital combination pH probes that had a gel-filled reference and a built-in temperature sensor (IntelliCAL™ PHC10105, Hach Systems). Values of pH were recorded every 15 min by a data logger (Hach Systems) connected via 5 m cables to the sensors and positioned in a waterproof housing above the water (Fig. 1). The pH probes were calibrated on site immediately before and after each deployment using three standards (pH 4.01, pH 7.00, and pH 10.01) as outlined by the National Institute of Standards and Technology.

### Light measurements

Photosynthetically active radiation (PAR) at the canopy height was measured every 15 min with autonomous submersible planar 2π Odyssey PAR sensors (Dataflow Systems), and then calibrated to a LI-193SA (LI-COR Biosciences) scalar 4π PAR sensor as described by Long et al. (2012). The PAR sensors

were inspected and cleaned for biofouling as described for the $O_2$ optodes.

**Salinity and turbidity measurements**

A submersible multiparameter probe (YSI-6600 V2) was mounted on the same frame holding the $pCO_2$ and pH sensors (Fig. 1) to record salinity and turbidity every 5 min at the canopy height. Before each deployment, salinity and turbidity sensors were calibrated with 10 mS $cm^{-1}$ and 50 mS $cm^{-1}$ solutions and with 0 and 100 NTU solutions, respectively.

Other environmental variables were calculated from data collected with the acoustic Doppler velocimeter. They included mean current velocity, current direction, significant wave height, and water depth (from water pressure readings).

**Shoot density, and aboveground and belowground biomass**

Seagrass characteristics were measured at the end of each sampling period. Shoot density was determined by counting individual shoots in eight quadrats (each 0.25 $m^2$) thrown randomly within 15 m of the instruments. Care was taken to stay outside the footprint of the aquatic eddy covariance measurements. Following a similar approach, six sediment cores (15.2 cm inner diameter) were randomly collected. The plant material was washed above a 1 mm sieve and the live parts were divided into aboveground and belowground biomass and weighed after drying at 60°C. The number of shoots per core was counted and the canopy height was determined as the average height of the three tallest leaves.

## *Data analysis*

**Eddy flux extractions**

Benthic $O_2$ fluxes were derived from the 32 Hz measured data following the protocol described below.

$O_2$ concentrations measured with the fast-responding microelectrode were calibrated against a predeployment "zero sample" reading in a sodium ascorbate solution and a concentration recorded during deployment with the autonomous $O_2$ optode (miniDOT). All 32 Hz data were subsequently averaged in groups of four to produce 8 Hz data, which reduces noise while providing sufficient resolution to contain the entire frequency spectrum carrying the flux signal (Berg et al. 2009). The continuous data were then divided in 15 min segments, and from each a flux was extracted using the software package EddyFlux version 2.0 (P. Berg unpubl.). Due to the relative large measuring height used (30 cm) and the substantial diurnal variations in $O_2$ concentration in the water column below the measuring point, a correction for $O_2$ stored in this volume improves the flux calculation (Rheuban et al. 2014*b*). The correction implicitly assumes that concentration changes in the bottom water below the measuring point is driven primarily by benthic activity (*see* "Discussion" section). The correction is included in the EddyFlux software and the benthic flux is calculated as:

$$\text{Benthic } O_2 \text{ flux} = \overline{w'C'} + \int_0^h \frac{dC}{dt}\, dz \quad (1)$$

where the overbar denotes averaging over the 15 min data segment, $w'$ and $C'$ the fluctuating components of the vertical velocity and the $O_2$ concentration, $h$ the measuring height, and $\frac{dC}{dt}$ the $O_2$ concentration change in time. The fluctuating components, $w'$ and $C'$, were determined as $w-\bar{w}$ and $C-\bar{C}$, respectively, where $w$ and $C$ are the measured values (8 Hz), and $\bar{w}$ and $\bar{C}$ are linear fits to $w$ and $C$ within each 15 min time interval. This approach for isolating $w'$ and $C'$ is commonly referred to as linear detrending (Lee et al. 2004; Berg et al. 2009). The constant slope of $\bar{C}$ was additionally used as an approximation of $\frac{dC}{dt}$ in the storage term in Eq. 1.

A thorough systematic data quality check was performed for each deployment after fluxes were calculated. This step is necessary as the microelectrodes are easily affected by floating debris that collides with the sensor tip, either destroying (breaking) it, or producing erroneous readings that can distort the flux calculation. For each 15 min time segment, the $O_2$ concentration and the cumulative flux were screened carefully for any abnormalities in the form of sudden jumps or changes that are distinguishable from natural turbulent fluctuations. Only $O_2$ fluxes that passed this quality check were used for further calculations. For more information on this process, see, for example, Berg et al. (2013). The 15-min fluxes were averaged to produce hourly fluxes (Hume et al. 2011).

Fluxes were extracted from both rotated and unrotated velocity data to examine if the instrument frames and the sensors were tilted relative to horizontal. Larger differences arising from the two data treatments were only found for a few hours where the water movements were dominated by wave motions. Because rotation of the velocity field can bias the flux if surface waves motions are present (Reimers et al. 2012) or if the current velocity is insignificant, the fluxes based on unrotated velocity data were used.

Due to the distance between the velocity and the $O_2$ sensors (~ 0.5 cm), and the limited response time of the $O_2$ sensors ($t_{90\%} < 0.4$ s), velocity and $O_2$ data are not aligned perfectly in time. In situations with well-defined current, flux estimates can often be improved by applying a time shift correction of the $O_2$ data relative to the velocity data (Fan et al. 1990; McGinnis et al. 2008; Lorrai et al. 2010). Conversely, in the presence of waves, this correction can introduce substantial biases in the flux estimate (Berg et al. 2015). Combined with a generally insignificant flux bias due to temporal sensor signal misalignment found in cospectral analysis of the vertical velocity and the $O_2$ concentration for selected deployments (Berg et al. 2013), this prompted us not to apply any time shift correction.

**Temperature effects on $pCO_2$**

The variation in $pCO_2$ due to changes in water temperature ($TpCO_2$) was calculated according to Takahashi et al. (2002) as:

$$TpCO_2 = pCO_{2mean} e^{0.0423(T - T_{mean})} \quad (2)$$

where $pCO_{2mean}$ is the mean $pCO_2$ value within each sampling period (April and June), $T$ is the varying temperature reading, and $T_{mean}$ is the mean temperature for each sampling period. $TpCO_2$ represents the $pCO_2$ variations around its mean due to temperature fluctuations alone.

**Averaging to hourly values**

All supporting variables including concentrations of $O_2$ and $pCO_2$, $TpCO_2$, temperature, PAR, pH, current velocity, salinity, and water depth were similarly averaged to hourly values to match the derived benthic $O_2$ fluxes. Gaps in the data (~ 10%) due to sensor malfunction or data download were filled by interpolation. A selection of these hourly values is shown in Figs. 2–3 for each of April and June.

**Metabolic characteristics**

For each full day of data (9 d in April and 12 d in June), the hourly fluxes were separated into daytime and night-time values using a PAR threshold of 10 $\mu$mol m$^{-2}$ s$^{-1}$, equivalent to ~ 1% of a clear-day maximum. The daytime and night-time hourly values were then used to calculate averaged daily respiration (R), gross primary production (GPP), and net ecosystem metabolism (NEM) as outlined by Hume et al. (2011):

$$R = \frac{1}{24}\left(\sum \text{flux}_{\text{dark}} + \frac{\sum \text{flux}_{\text{dark}}}{h_{\text{dark}}} h_{\text{light}}\right) \quad (3)$$

and

$$GPP = \frac{1}{24}\left(\sum \text{flux}_{\text{light}} + \frac{|\sum \text{flux}_{\text{dark}}|}{h_{\text{dark}}} h_{\text{light}}\right) \quad (4)$$

and

$$NEM = \frac{1}{24}\left(\sum \text{flux}_{\text{light}} + \sum \text{flux}_{\text{dark}}\right) \quad (5)$$

where $\text{flux}_{\text{dark}}$ and $\text{flux}_{\text{light}}$ are the respective night-time and daytime hourly fluxes within each day (separated by the PAR threshold of 10 $\mu$mol m$^{-2}$ s$^{-1}$), and $h_{\text{dark}}$ and $h_{\text{light}}$ are the number of night-time and daytime hours ($h_{\text{dark}} + h_{\text{light}} = 24$). Averages of these metabolic numbers for each of April and June are shown in Fig. 4.

**Diel cycle and hysteresis**

To evaluate the typical or average diel cycle, hourly values were binned by the hour of day for each of the 2 months. The data are shown in Fig. 5. Similarly, the 24 hourly binned water column $pCO_2$ values for each month were plotted as a function of the concurrent $O_2$ concentrations (in percent of saturation) in Fig. 6a,b. Relying on the same unit, Fig. 6c,d shows a more direct presentation of the relationship between dissolved inorganic carbon (DIC) and $O_2$ water column concentrations. The $O_2$ concentrations were measured directly (Figs. 2–3), while the DIC concentrations were estimated from measured hourly $pCO_2$, temperature, and salinity data (Figs. 2–3; Table 1). In the absence of riverine inputs as indicated by a near-constant salinity (Table 1) and low watershed nutrient inputs to South Bay (McGlathery et al. 2007), TA required for this calculation was taken from regional surface-water data measured and fitted for the Mid-Atlantic Bight by Cai et al. (2010) as TA = 670.6 + 46.6 $S$ $\mu$mol kg$^{-1}$, where $S$ is the salinity in ppt. DIC concentrations were then calculated using the CO2SYS MATLAB 1.1 package (Lewis et al. 1998; Van Heuven et al. 2011; Orr et al. 2015), and the Mehrbach carbonic acid and bicarbonate dissociation coefficients as refitted by Dickson and Millero (1987). Seawater density was used in unit conversions of DIC and alkalinity. Water column silicate and phosphate concentrations were assumed to be low (VCR LTER water-quality database; www.vcrlter.virginia.edu), and thus not affecting this calculation.

**Photosynthesis-irradiance curves**

Measured hourly daytime $O_2$ fluxes for each of the 2 months were used to determine photosynthesis-irradiance (P-I) relationships for the seagrass meadow using the standard P-I function proposed by Jassby and Platt (1976) and modified to also account for respiration:

$$\text{Benthic O}_2\text{ flux} = P_{\max} \tanh\frac{I}{I_S} - R_I \quad (6)$$

where $P_{\max}$ is the maximum photosynthetic rate, $I$ the measured light (PAR) at canopy height, $I_s$ the light saturation constant, and $R_I$ is the respiration. The functions for April and June for fitted values of $P_{\max}$, $I_s$, and $R_I$ are shown in Fig. 7.

**Effects of $CO_2$ and $O_2$ concentrations on photosynthesis**

The 4.5-fold variation in water column $pCO_2$ (193–859 ppmv) and the 2.2-fold variation of the $O_2$ concentration (172–377 $\mu$mol L$^{-1}$) encountered during the peak growing season, and the concurrent daytime $O_2$ fluxes, were used to examine if in situ seagrass photosynthetic production was stimulated at high $CO_2$ levels (Zimmerman et al. 1997; Borum et al. 2016), inhibited at high $O_2$ levels (Raven and Larkum 2007; Mass et al. 2010; Buapet et al. 2013), or both. Because $CO_2$ stimulation would be most pronounced at high light intensities where light limitation diminishes (Palacios and Zimmerman 2007; Alexandre et al. 2012), only data above the 50% light saturation line (Fig. 7) were included in the analysis. Using the ratio between hourly $pCO_2$ values and $O_2$ concentrations ($pCO_2$:$O_2$)

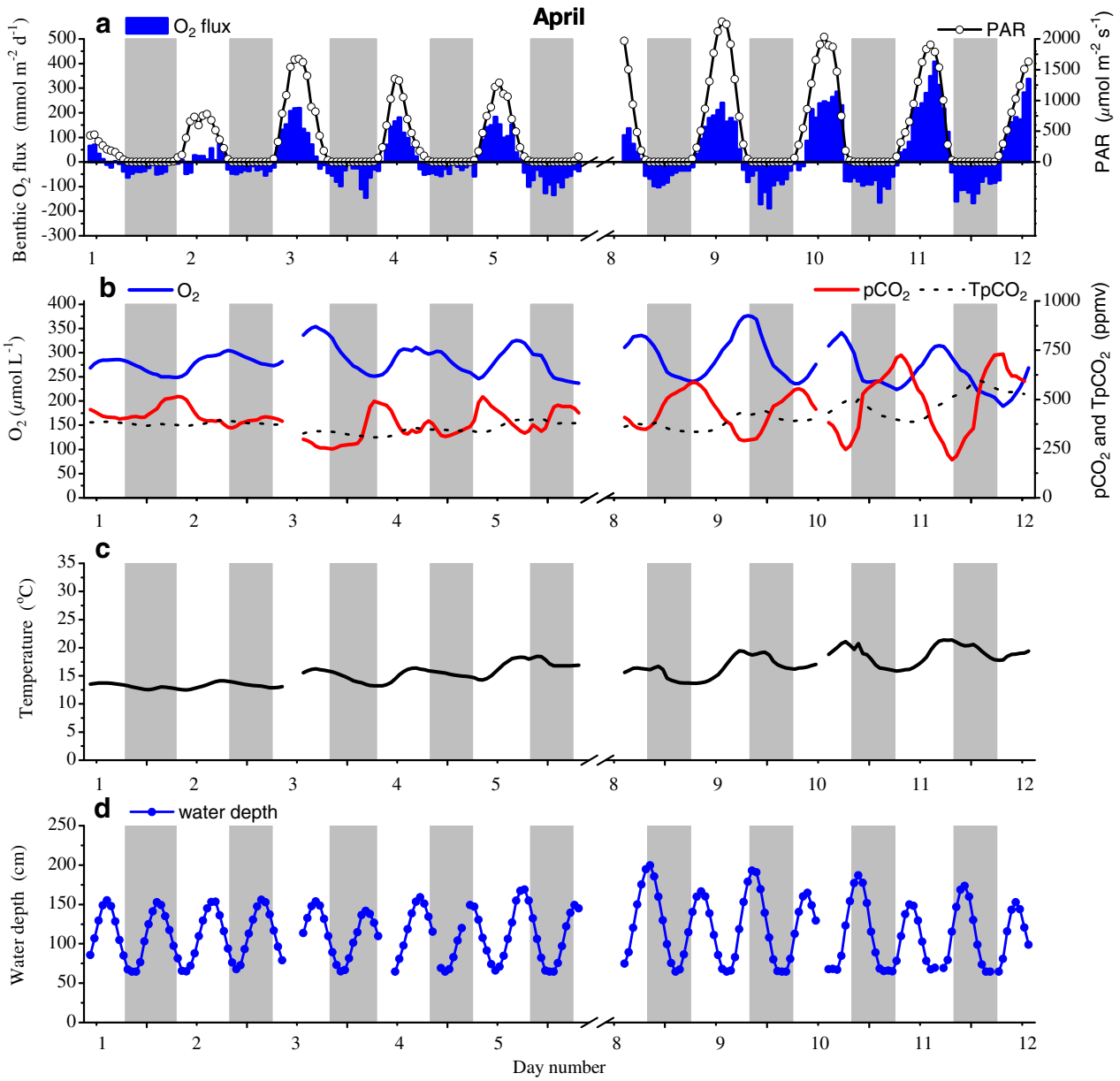


**Fig. 2.** Hourly values for 12 sampling days in April. Gray shading marks night-time. (**a**) Aquatic eddy covariance $O_2$ fluxes between the seagrass meadow and the overlying water (blue bars, positive values represent a release), and PAR at canopy height (circles/line). (**b**) Concentration of $O_2$ (blue line), $pCO_2$ (red line), and $TpCO_2$ (dotted line, represents variations in $pCO_2$ due to temperature changes). (**c**) Temperature at canopy height. (**d**) Water depth.

to distinguish between favorable and unfavorable conditions for seagrass photosynthesis, the data were separated into 25$^{th}$ percentiles. The upper and the lower percentiles of the hourly $pCO_2$:$O_2$ ratios, and the corresponding values of the $pCO_2$ and $O_2$ concentrations, PAR, and benthic $O_2$ flux for April and June are shown in Fig. 8.

## *Results*

### Site characteristics

Variations in environmental parameters and seagrass characteristics during the study period (Table 1) were consistent with long-term measurements (VCR LTER water-quality database; www.vcrlter.virginia.edu). Specifically, salinity was near constant with a maximum variation between –0.4 and 0.6 ppt from a mean of 31.9 ppt for April and between –1.6 and 1.0 ppt from a mean of 30.3 ppt for June. Water temperature varied from 12.5°C to 21.4°C in April and from 24.0°C to 30.9°C in June. The larger variation in April was explained by an increase through the measurement period that overlaid the diel variations (Fig. 2c). Water depth was similar for the 2 months with a mean of ~ 1.15 m overlaid by a tidal variation of similar magnitude. Average light (PAR) reaching the seagrass canopy was 21% less in June than in April, presumably due to

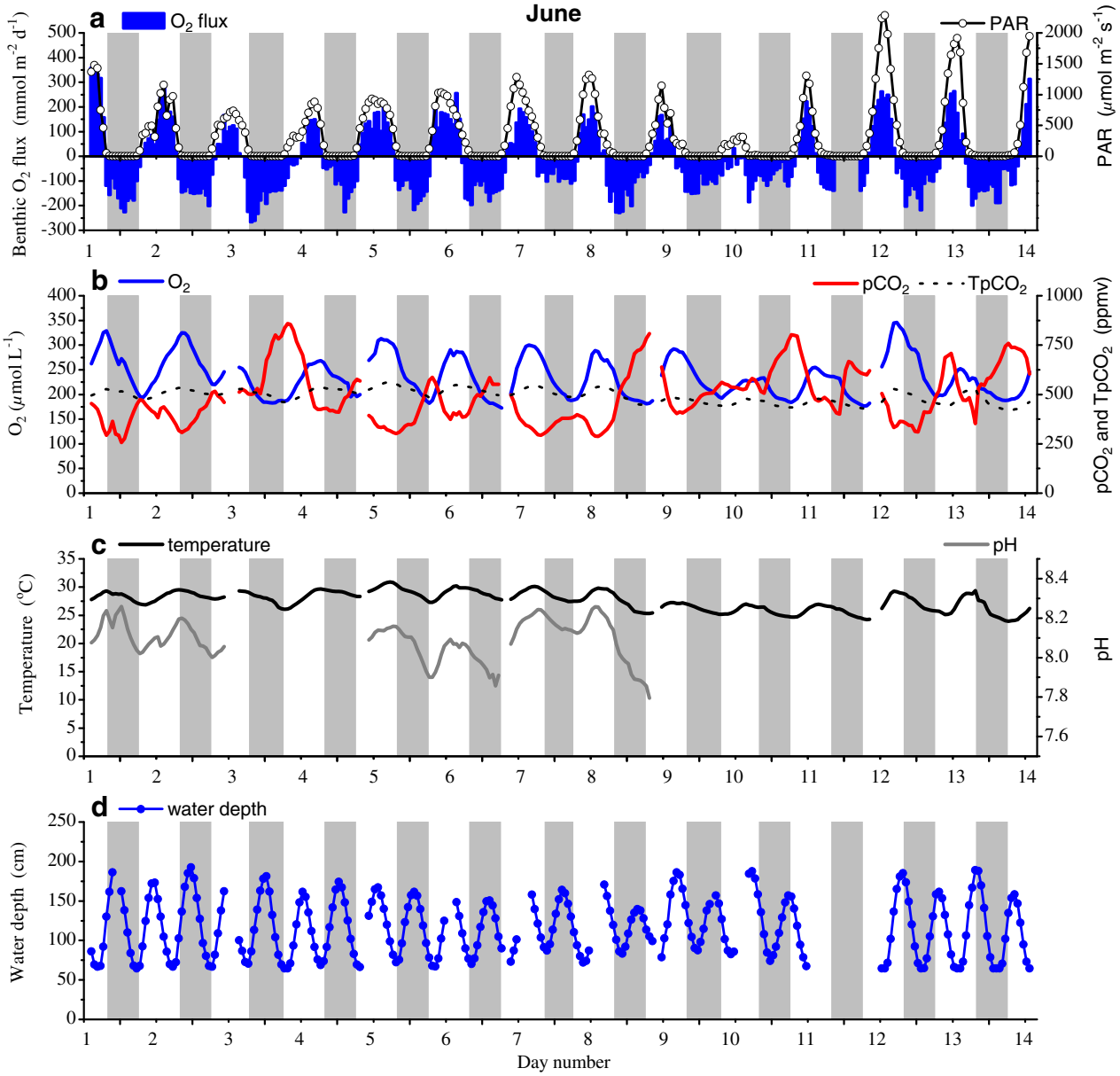


**Fig. 3.** Hourly values for 14 sampling days in June. Gray shading marks night-time. (**a**) Aquatic eddy covariance $O_2$ fluxes between the seagrass meadow and the overlying water (blue bars, positive values represent a release), and PAR at canopy height (circles/line). (**b**) Concentration of $O_2$ (blue line), $pCO_2$ (red line), and $TpCO_2$ (dotted line, represents variations in $pCO_2$ due to temperature changes). (**c**) Temperature (black line) and pH (gray line) at canopy height. (**d**) Water depth.

substantially higher turbidity in June (214 vs. 33 NTU; Table 1). Water column concentrations of $O_2$ and $pCO_2$ over the diel cycle exhibited similar variations in each of the 2 months.

Between April and June, aboveground biomass and seagrass shoot length increased by almost 50%, while shoot density declined by 27% (Table 1). This implies that new shoot formation decreased while existing shoots grew from April to June, possibly in response to higher mean temperatures (16.0°C vs. 27.6°C). Belowground biomass increased by 23% as expected as the growing season progressed.

### Benthic $O_2$ fluxes and water column characteristics

The derived hourly $O_2$ fluxes (Figs. 2a, 3a) showed a clear diel pattern throughout both measurement periods. Specifically, the hourly $O_2$ flux varied from –188 to 408 mmol $m^{-2}$ $d^{-1}$ in April and –267 to 359 mmol $m^{-2}$ $d^{-1}$ in June, with negative values representing benthic uptake. It was also evident that days with high PAR levels at the seagrass canopy height (Figs. 2a, 3a) triggered larger positive benthic fluxes relative to days with less light. Variations in water column concentrations of $O_2$ and $pCO_2$ exhibited a similarly distinct diel pattern with

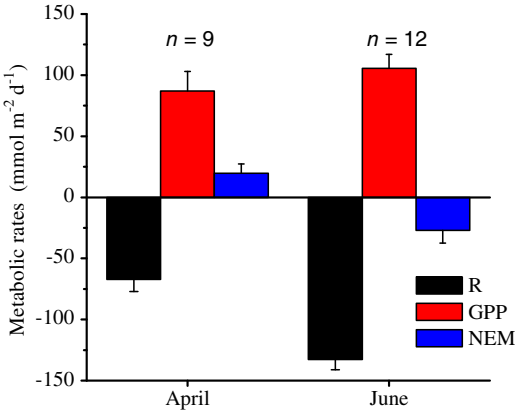


**Fig. 4.** Averaged daily respiration (R), gross primary production (GPP), and net ecosystemmetabolism (NEM) for April and June (error bars represent SE). NEM was significantly different from 0 for both months ($p$ = 0.03 in both months) and indicates a trophic shift from autotrophy to heterotrophy.

24 h oscillations of the two constituents being out of phase. Variations in water temperature had a clear, but relatively small, diel imprint with an average fluctuation of ~ 3°C. Variation in the intermittent pH measurements in June (Fig. 3c) exhibited diel variations of 0.2–0.4, with lowest pH values occurring near dawn following night-time net respiration. Measured pH was inversely related to $pCO_2$ variations consistent with the expected relationship from seawater $CO_2$ system thermodynamics (data not shown).

### Metabolism

Averages of the daily metabolic rates for April and June (Fig. 4) reflect substantial changes through the growing season. NEM switched from being positive in April to negative in June ($p$ = 0.03) while R increased twofold. No significant difference was found between GPP for the 2 months ($p$ = 0.34).

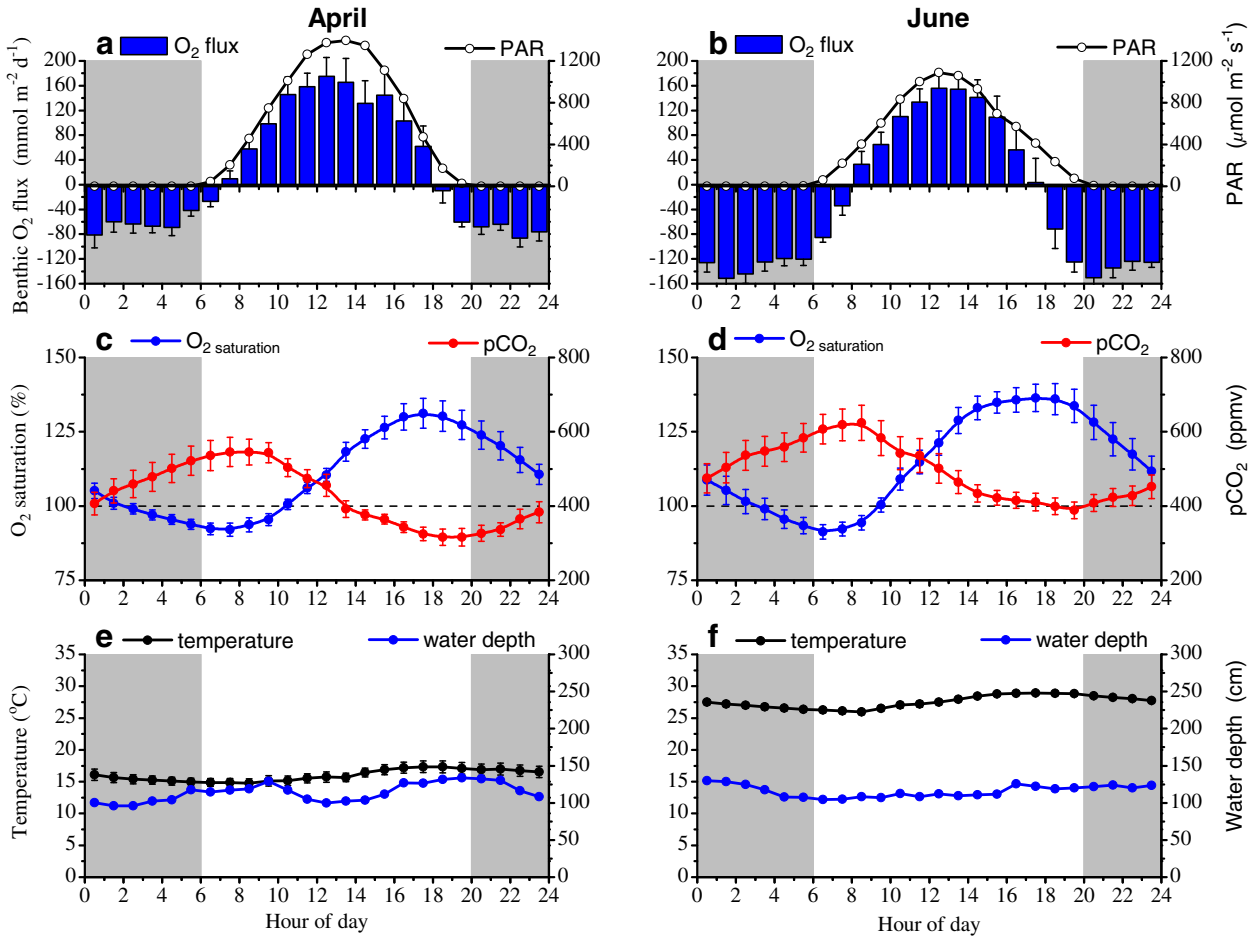


**Fig. 5.** Hourly values binned by the hour of day for April and June. (**a**, **b**) Aquatic eddy covariance $O_2$ fluxes between the seagrass meadow and the overlying water (blue bars, positive values represent a release), and PAR at canopy height (circles/line). (**c**, **d**) Concentration of $O_2$ in percent of saturation (blue line) and $pCO_2$ (red line). The dashed line represents 100% oxygen saturation and air–sea equilibrium of $CO_2$. Values above this line for either $O_2$ or $pCO_2$ indicate a release to the atmosphere. (**e**, **f**) Temperature (black line) and water depth (blue line). For both months, temperature varied by less than 3°C. Error bars represent SE ($n$ = 9 for April and 12 for June).

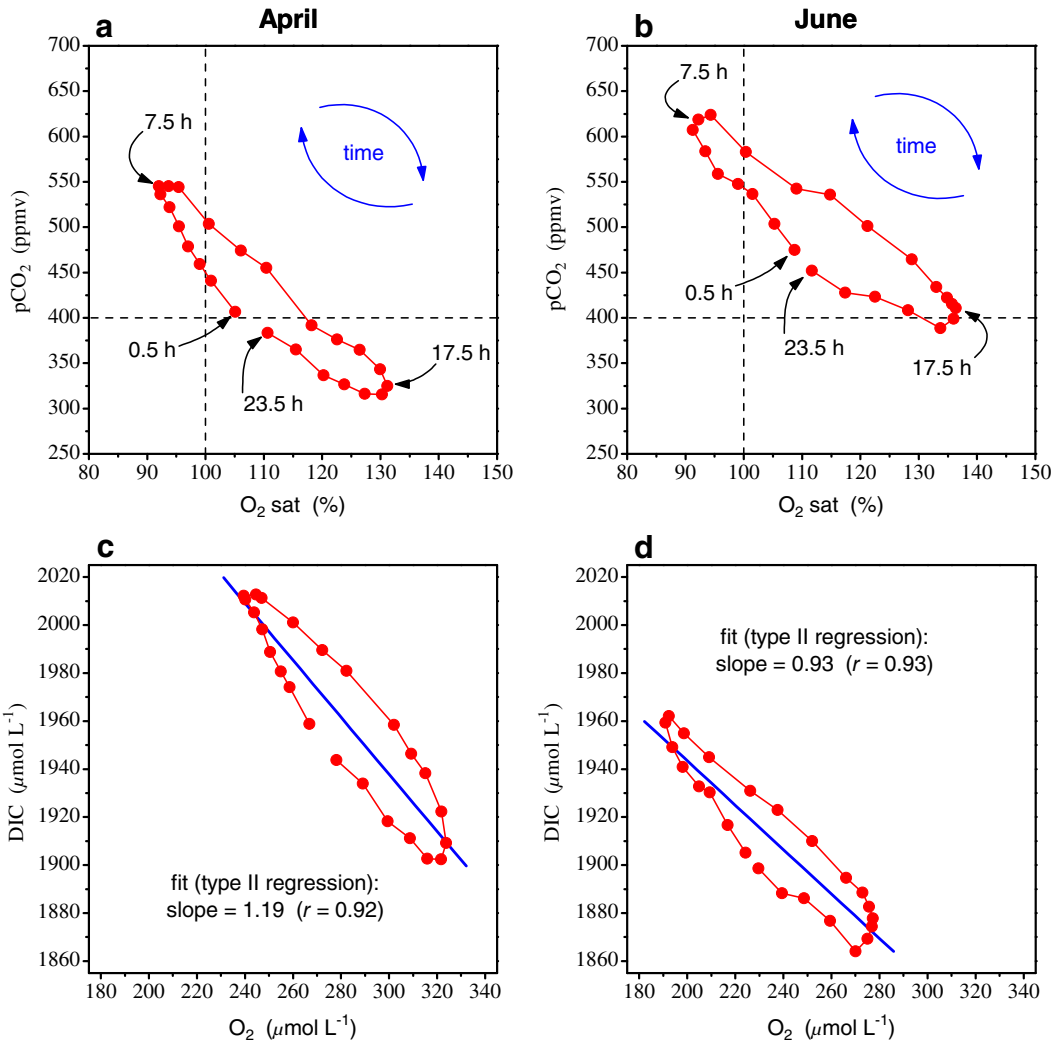


**Fig. 6.** Binned hourly $pCO_2$ values (from Fig. 5) plotted as function of $O_2$ concentration (percentage of saturation) for (**a**) April and (**b**) June. Dotted lines represent water column equilibrium with the atmosphere. Estimated binned hourly concentration of DIC (see text for details) as a function of $O_2$ concentration for (**c**) April and (**d**) June. The linear type II regression lines have slopes of 1.19 and 0.93 for April and June, respectively. Explanations for the pronounced hysteresis effects seen in all panels are given in the text.

### Binned $O_2$ fluxes and water column characteristics

The distinct diel variation in the benthic $O_2$ fluxes and water column concentrations becomes even more evident when the hourly data for the 9 and 12 full days in April and June, respectively, (Figs. 2–3) are binned by the hour of day (Fig. 5). The binned $O_2$ flux and PAR data (Fig. 5a,b) for the 2 months exhibited a near-perfect distribution around mid-day with PAR being 21% smaller in June likely due to the substantially higher turbidity (Table 1). Daytime $O_2$ fluxes for April and June were similar, while night-time fluxes were substantially larger in June as also reflected in the averaged metabolic numbers (Fig. 5a,b).

The averaged diel variations in water column temperature were small, ranging between 14.7°C and 17.3°C in April and 25.9°C and 28.9°C in June (Fig. 5e,f). The binned water depth varied within 16.5% and 11.0% from the means for the 2 months, respectively, indicating that our data were distributed relatively evenly over the tidal cycle. Water column concentrations of $O_2$ and $pCO_2$ described near-perfect sinusoidal variations that were out of phase by almost 180° (Fig. 5c,d). An offset from an exact 180° phase shift becomes evident when plotting the hourly binned $pCO_2$ values as a function of their corresponding $O_2$ concentrations (Fig. 6a,b). A clear hysteresis was identified for each month, and was similarly present when depicturing estimated DIC concentrations vs. $O_2$ concentrations using the same unit (Fig. 6c,d). Type II linear regressions of the data gave regression lines with slopes of 1.19 and 0.93 for April and June, respectively (Fig. 6c,d).

### P-I relationships and $CO_2$ and $O_2$ limitation of photosynthesis

The P-I curves defined by Eq. 6 and fitted to the hourly daytime $O_2$ fluxes for each of April and June (Fig. 7) reached near-saturation levels of 89% and 99%, respectively. Moreover, the

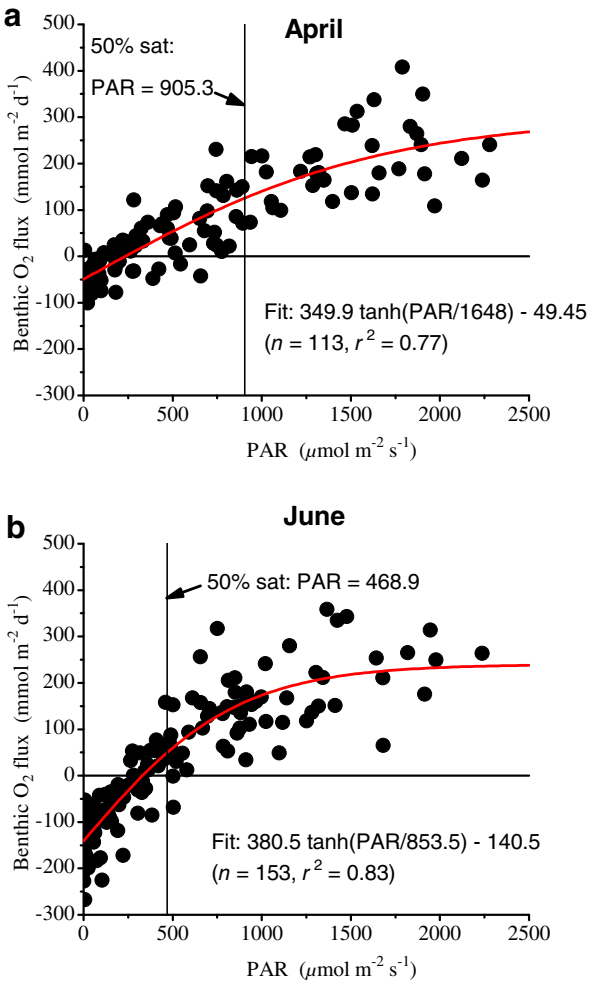


**Fig. 7.** Photosynthesis-irradiance (P-I) curves fitted to hourly daytime fluxes, indicating 89% and 99% light saturation at the highest PAR levels for April (**a**) and June (**b**). 50% saturation was found for 905.3 $\mu$mol $m^{-2}$ $s^{-1}$ in April and 468.9 $\mu$mol $m^{-2}$ $s^{-1}$ in June, a difference that may be related to the higher shoot density in April (Table 1). Data above the 50% saturation line were used to examine effects of coinciding high $pCO_2$ values and low $O_2$ concentrations on photosynthesis (*see* Fig. 8).

two curves had light compensation points of 235 and 311 $\mu$mol $m^{-2}$ $s^{-1}$, a difference of 32% that is likely explained by the larger respiration in June (Figs. 4–5).

Data above the 50% light saturation line (Fig. 7), for which any photosynthetic stimulation due to high $CO_2$ and/or low $O_2$ concentrations would be most pronounced (Palacios and Zimmerman 2007; Alexandre et al. 2012), showed substantial differences when grouped in 25$^{th}$ percentiles based on their ratio of $pCO_2$:$O_2$ (Fig. 8). Specifically, differences between ratios in the lower and the upper percentiles equaled a factor of 2.1 in April (Fig. 8a) and 2.5 in June (Fig. 8f). The corresponding $pCO_2$ values and $O_2$ concentrations were different by factors of 1.7 and 1.8 for $pCO_2$ and 0.80 and 0.72 for $O_2$ (Fig. 8b,c,g,h). On the contrary, light levels for the two percentiles (Fig. 8d,i) were not significantly different ($p$ = 0.74 for April, $p$ = 0.053 for June). As a result, the lack of difference between the average benthic $O_2$ fluxes ($p$ = 0.64 for April, $p$ = 0.53 for June; Fig. 8e,j) indicates that the seagrass meadow photosynthesis, measured under naturally varying field conditions, was not stimulated at high $pCO_2$ and low $O_2$ concentrations, nor limited at low $pCO_2$ and high $O_2$ concentrations.

## Discussion

Seagrass meadows, salt marshes, and mangroves that line coasts worldwide are considered important contributors to blue carbon sequestration and storage (Duarte et al. 2005, 2013*b*). Recent estimates have suggested that the carbon retention of these aquatic ecosystems is up to 40 times higher than that of terrestrial forests per unit area, and when accounting for the larger areal coverage of forests, that the two ecosystem types store and sequester comparable amounts of carbon per year (Mcleod et al. 2011). Although the magnitudes of these estimates are uncertain, and currently being debated and re-evaluated (Johannessen and Macdonald 2016; Macreadie et al. 2018; Oreska et al. 2018), the consensus is that coastal vegetated ecosystems play an important role in binding carbon globally, and thus, in mitigating anthropogenic $CO_2$ emissions.

Seagrass meadows account for up to half of the global carbon sequestration and storage by coastal vegetated ecosystems (Mcleod et al. 2011). Yet, their complex and dynamic metabolism and its controls are not fully understood. For example, it remains an open question whether seagrass production will be stimulated by elevated $CO_2$ concentrations in future oceans (Ruesink et al. 2015; Collier et al. 2018; Pacella et al. 2018). In this context, we made high temporal-resolution measurements in situ of seagrass meadow metabolism and supporting variables through 21 full days during peak growing season. By using the aquatic eddy covariance technique (Berg et al. 2003*a*) and state-of-the-art autonomous submersible $O_2$, $pCO_2$, and light sensors, we produced an extensive data set on whole-system seagrass metabolism and its controls under naturally varying field conditions.

### Tight coupling of metabolic processes

Our in situ data show a strong light-dependency of seagrass metabolism on multiple time scales, and are in agreement with other shallow macrophyte-dominated ecosystem studies in both freshwater and marine environments (Pedersen et al. 2013). This tight coupling is, for example, reflected in the hourly values of benthic $O_2$ exchange which showed a strong diel pattern (Figs. 2a, 3a), ranging from an uptake of –267 mmol $m^{-2}$ $d^{-1}$ to a release of 408 mmol $m^{-2}$ $d^{-1}$. These fluxes and their dynamics are largely in agreement with our previous aquatic eddy covariance measurements in the same seagrass meadow in South Bay (Fig. 1) (Hume et al. 2011; Rheuban et al. 2014*a*,*b*; Berg et al. 2017).

Substantial diel covariance was similarly measured in the water column concentration of $O_2$ and $pCO_2$ (Figs. 2b, 3b), with values ranging from 173 to 377 $\mu$mol $L^{-1}$ and 193 to 859 ppmv,

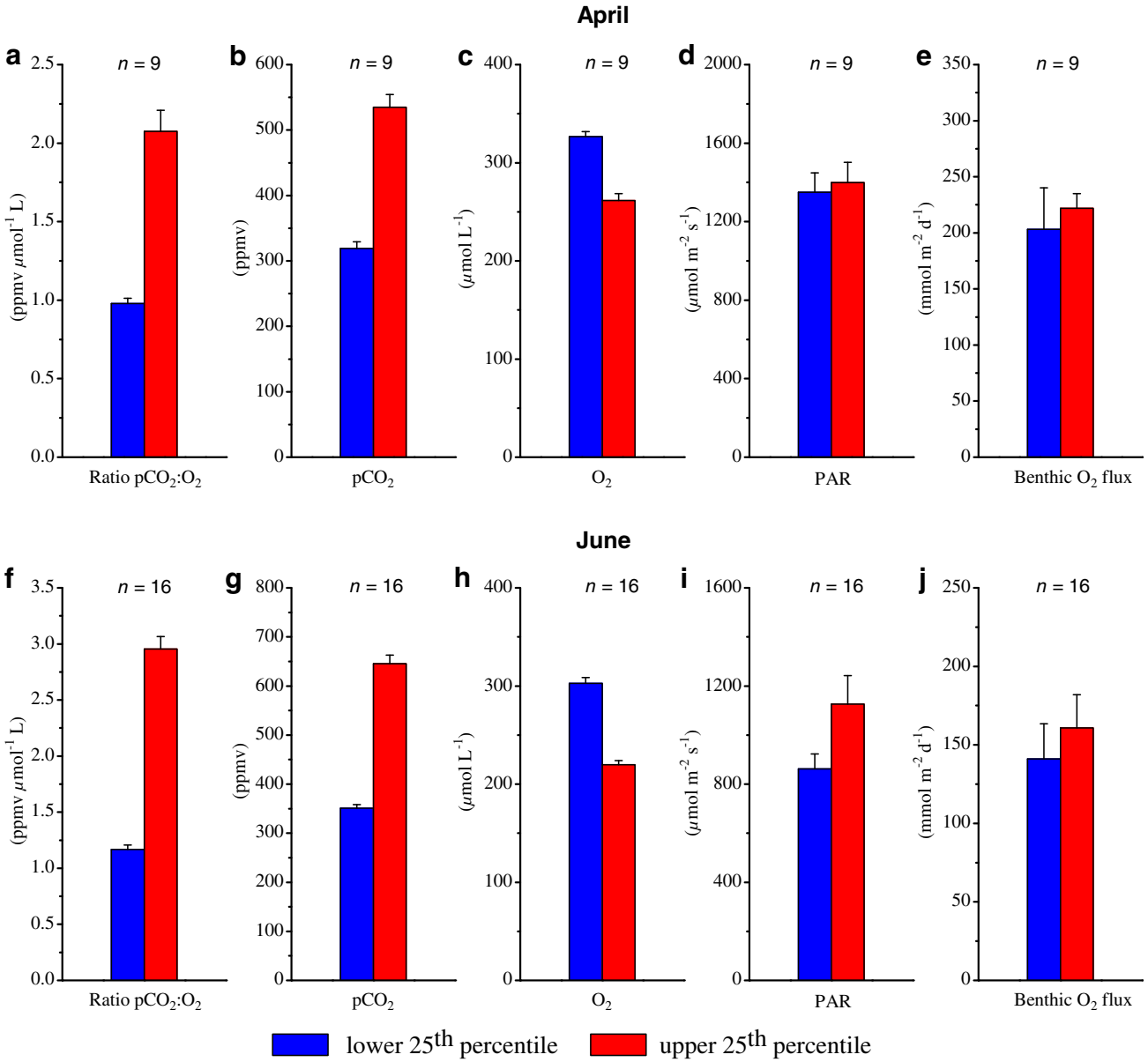


**Fig. 8.** Potential effects of concurrent high $pCO_2$ values and low $O_2$ concentrations on photosynthesis. Data above the 50% saturation line in Fig. 7 were grouped in lower and upper 25$^{th}$ percentiles using the $pCO_2$:$O_2$ ratio. The mean of the upper percentile was 212% larger than the lower percentile for April (**a**). The similar number for June was 253% (**f**). These differences arose from $pCO_2$ values that differed by 168% and 184% between the two percentiles for the 2 months (**b**, **g**), combined with the equivalent numbers for the $O_2$ concentrations of 80% and 73% (**c**, **h**). Differences in PAR (**d**, **i**) for the lower and upper 25$^{th}$ percentiles were not significant ($p$ = 0.74 for April, $p$ = 0.053 for June), and the same was found for the benthic $O_2$ flux (**e**, **j**; $p$ = 0.64 for April, $p$ = 0.53 for June). Despite the significant variations in $pCO_2$ values and $O_2$ concentrations encountered in situ during the most productive spring and summer months, no stimulation of photosynthetic production was found at high $pCO_2$ values and low $O_2$ concentrations (error bars represent SE).

respectively. The 4.5-fold variation in $pCO_2$ was observed despite buffering by the carbonate system, and was due largely to plant metabolism rather than to direct temperature effects (Eq. 2, Figs. 2b, 3b). These diel $pCO_2$ fluctuations are consistent with the few other studies where time series of $pCO_2$ in seagrass meadows have been recorded. For example, in *Thalassia testudinum* dominated meadows in subtropical Florida, $pCO_2$ was measured over a few diel cycles and ranged from 260 to 497 ppmv in Florida Bay (Yates et al. 2007) and from 379 to 1019 ppmv in St. Joseph Bay (Challener et al. 2016). In a *Posidonia oceanica* meadow in the western Mediterranean Sea, 72 h of $pCO_2$ measurements showed a range from 105 to 507 ppmv (Hendriks et al. 2014). With increasing atmospheric $CO_2$ and resulting ocean acidification, it is expected that the carbonate system in seagrass meadows will be less able to buffer natural fluctuations, and as a result, that extreme events of

high $pCO_2$ and low pH will become more frequent (Pacella et al. 2018).

Day-to-day variations in seagrass meadow metabolism and water column concentrations were caused primarily by external drivers such as changes in light availability from variable cloud cover. For example, the day with the least light at canopy height during the entire study period (day 10 in June, Fig. 3a) was the only day when seagrass meadow respiration overpowered photosynthetic production during the daytime hours and gave a net $O_2$ uptake (Fig. 3a). The effect of this rather atypical situation coincided with equally small variations in water column $O_2$ concentrations and $pCO_2$ (Fig. 3b). Other examples of this relationship can easily be identified in the 21 d data record (Figs. 2–3), and indicate a tight coupling between metabolic activity in the seagrass meadow and variations in the water column (see more details below). Furthermore, the absence of larger and more sudden temperature changes through the measurement periods (Figs. 2c, 3c) suggests that oceanic tidal exchange or input of drainage water from surrounding tidal channels and salt marshes are not major drivers of variations in water column characteristics at this site.

The dynamic but repetitive patterns identified in Figs. 2–3 makes the entire data set an excellent platform for relating whole-system metabolism for a temperate seagrass meadow during the peak growing season to water column $O_2$ and $CO_2$ concentrations and other environmental variables.

**Switch between autotrophy and heterotrophy**

The average of all daily metabolic rates (Eqs. 3–5; Fig. 4), R, GPP, and NEM was in the range of those reported for temperate seagrass meadows (Duarte et al. 2010). However, as a rather surprising observation, NEM switched from being significantly positive in April (20 mmol $m^{-2}$ $d^{-1}$, $p = 0.033$) to significantly negative in June (–27 mmol $m^{-2}$ $d^{-1}$, $p = 0.025$). This trophic shift from autotrophy to heterotrophy was likely driven by a twofold increase in R (Fig. 4) as biomass increased by a third (Table 1) and the average water temperature almost doubled, from 16.0°C in April to 27.6°C in June (Table 1). This change happened while GPP only increased by ~ 20% (Fig. 4). Relating the increase in R directly to temperature translates to a $Q_{10}$ value of 1.8 for the whole benthic system respiration, including seagrass, epiphytes, and sediment, which is not far from the range of 2.0–2.7 for dark leaf respiration measured in the lab for tropical seagrass species (Pedersen et al. 2016).

We have previously observed transitions from autotrophy to heterotrophy, or a shift from the seagrass meadow being a sink to a source of carbon, based on aquatic eddy covariance measurements and modeling for this mature seagrass meadow (Rheuban et al. 2014*a*,*b*). However, in these earlier studies, the switch occurred later in the summer, in August, rather than in June. This difference in timing may either reflect natural variations or it may be an early sign of a severe seagrass dieback that was observed late in the summer of 2015. Our measured seagrass densities dropped from 316 $m^{-2}$ in April to 230 $m^{-2}$ June (Table 1) and appear to support the latter explanation. Unusually high water temperatures also were recorded in June, with a maximum of 31°C (Table 1) and exceeding the temperature stress threshold of 28°C proposed by Staehr and Borum (2011) in 46% of the total deployment time. The *Z. marina* populations in Virginia are growing near the southern distribution limit along the North American coast and may be especially vulnerable to marine heat waves. Other studies have related seagrass dieback in the lower Chesapeake Bay to summer time high temperatures that exceed the plants physiological tolerance and capacity to adapt to heat (Moore and Jarvis 2008; Moore et al. 2012). Laboratory experiments with seagrass have shown the clear negative effects of high temperatures by reducing productivity and protein/enzyme synthesis, increasing mortality, and inducing anoxia in plant meristems (Greve et al. 2005; Moore and Jarvis 2008; Hammer et al. 2018).

Regardless of what triggered the early switch from autotrophy to heterotrophy, the year-to-year difference exemplifies how dynamic the metabolism of seagrass meadows can be, also on a time scale larger than that covered in this study. Together, the metabolic results obtained here and those found in our earlier eddy covariance work in South Bay (Hume et al. 2011; Rheuban et al. 2014*a*,*b*; Berg et al. 2017) show how easily inaccurate conclusions about the trophic status of a seagrass meadow can be drawn if only limited measurements are made that do not capture the natural variation over multiple time scales characteristic of the benthic system. The early switch documented here underlines that determination of the trophic status, even within one season, should be based on temporally well-distributed measurements.

**Hysteresis**

The binned hourly water column concentration of $O_2$ and $pCO_2$ for both months (Fig. 5c,d) describes a near-perfect sinusoidal variation that at first appears to be perfectly out of phase. However, a close inspection of the two variables reveals that their optima (minima and maxima) in both months are offset by ~ 2 h from one another. This offset results in a clear hysteresis when the binned $pCO_2$ values are plotted against the binned $O_2$ concentrations (Fig. 6a,b), and similarly, when $O_2$ and DIC concentrations are compared after being converted to the same unit of $\mu$mol $L^{-1}$ (Fig. 6c,d). We have identified three possible independent mechanisms that can lead to this hysteresis.

First, seagrass leaves (and roots) can store considerable amounts of both $CO_2$ and $O_2$ (Greve et al. 2003; Borum et al. 2007; Pedersen et al. 2013). This intermediate step, or delay, between when the $CO_2$ and $O_2$ are produced or consumed, and when the two constituents are exchanged with the water column can lead to hysteresis. Second, due to the carbonate system buffering, the driving partial pressure difference for air–water gas exchange of $CO_2$ is easily an order of magnitude smaller than that of $O_2$ (Dai et al. 2009; Zhai et al. 2009). This difference slows down the re-equilibration of $CO_2$ relative to that of $O_2$ between the water column and the air above, and

combined with the diurnally varying exchange of $CO_2$ and $O_2$ between the seagrass meadow and the water column can likewise result in hysteresis. Third, all primary redox reaction processes that can be responsible for organic matter degradation in the sediment (oxic decomposition, denitrification, manganese reduction, iron reduction, sulfate reduction, and methanogenesis) produce $CO_2$ (Canfield et al. 1993; Van Cappellen and Wang 1996; Berg et al. 2003*b*). This results in a $CO_2$ surplus in the sediment that is released to the water column through vertical transport processes such as molecular diffusion, bioturbation, and bioirrigation (Berner 1980; Boudreau 1997). If the water column $CO_2$ concentration is near constant, so is this release. However, at diurnally oscillating $CO_2$ concentrations as documented in this study (Fig. 5), there will be periods in each diel cycle where there is a reversed flux of $CO_2$ into the sediment from the water column. This pattern can similarly create hysteresis as documented here (Fig. 6).

**Seagrass metabolism and water column concentrations**

Using the binned hourly $O_2$ fluxes (Fig. 5a,b) in a simple mass-balance calculation reveals that benthic metabolism explains about 60% of the diel variation measured in water column concentrations of $O_2$ and $pCO_2$. This result is largely in agreement with other studies of seagrass meadow metabolism (Semesi et al. 2009; Hendriks et al. 2014). However, this simplified mass balance disregards several smaller contributions, including production and consumption in the water column itself, tidal and wind-driven horizontal advective transport, and air–water gas exchange.

Traditional bottle incubations are an imperfect measure of water column GPP because they are typically performed during a few mid-day hours, at peak sunlight, and represent a maximum potential production. As such, they are not directly comparable with the daily averages of GPP for the seagrass meadow we report here (Fig. 4). However, previous dark bottle incubations from our site gave an average R value of $-21$ mmol $m^{-2}$ $d^{-1}$ for June (Rheuban 2013), amounting to 16% of that we measured by eddy covariance (Fig. 4). This suggests that only a small fraction of the measured water column variations in $O_2$ and $CO_2$ concentrations arises from activity in the water column itself. Our site is located in the center of the South Bay seagrass meadow (Fig. 1). Despite this, horizontal advective inputs from surrounding tidal channels, salt marshes, and the ocean may at times affect water column concentrations at our site. Given the mean water depth of ~ 1 m and a ~ 1 m tidal range (Table 1; Figs. 2–3), these contributions are likely most pronounced at high and low tide, and during times with strong wind-driven currents. Beyond that, their magnitude and temporal dynamics are impossible to assess with the data at hand and require further studies. However, we note that the water column, when averaged over the diel cycle (Fig. 5c,d), was supersaturated with both $O_2$ and $CO_2$, indicating some periodic influence by horizontal advection, an argument that has been made previously (Ruesink et al. 2015). Due to inherently large uncertainties associated with quantifying air–water gas exchange coefficients (Raymond and Cole 2001; Borges et al. 2004), we abstained from estimating the air–water fluxes in this study.

The close to 1:1 mol-to-mol elemental stoichiometric relationship that was found in the linear regressions of DIC and $O_2$ concentrations for both April and June (Fig. 6c,d) lines up well with the flux ratios between the two constituents of 0.8–1.2 reported for different benthic environments (Glud 2008). This result was obtained despite uncertainties associated with our first-order estimate of the DIC concentration. There are no river inputs to the VCR lagoons and long-term studies indicate that stream and land runoff of freshwater and nutrients to the study site are negligible (McGlathery et al. 2007). With seagrass metabolism being the main driver of diel variations in water column concentrations of DIC and $O_2$, the relationship can be viewed as an integrated measure of how $O_2$ dynamics and carbon transformations are related for the seagrass meadow through a set of complex processes. With the rapid development of new user-friendly autonomous underwater sensors for $O_2$, $pCO_2$, pH, and TA, we expect that more estimates along these lines will be reported for a variety of benthic environments. Comparisons of such mol-to-mol elemental stoichiometric relationships for different systems may reveal important differences between ecosystems and their functioning.

**$CO_2$ and $O_2$ concentrations and seagrass metabolism**

The fitted P-I curves (Fig. 7) represent whole-system P-I responses for the seagrass meadow when exposed to naturally varying field conditions. For both months, benthic net production reached near-light-saturation levels (89% and 99%, respectively) where stimulation of seagrass photosynthesis by elevated $CO_2$ water column concentrations is expected to be most pronounced (Pedersen et al. 2013). Additionally, $pCO_2$ values varied widely during the study period, ranging from 193 to 859 ppmv (Figs. 2–3), with the latter value overlapping $pCO_2$ levels used in IPCC 2013 ocean acidification scenarios (800–1200 ppmv by 2100; Stocker 2014). This 4.5-fold variation in $pCO_2$ was complemented by a conversely varying $O_2$ concentration between 173 and 377 $\mu$mol $L^{-1}$, so that high $pCO_2$ values were accompanied by low $O_2$ concentrations, and vice versa (Figs. 2–3). Because of this pattern, and because high $O_2$ concentration levels inhibited seagrass photosynthesis (Mass et al. 2010), our in situ data are well suited for examining whether seagrass photosynthesis is affected by realistic and naturally varying $CO_2$ and $O_2$ concentrations in the water column.

Enhancement of seagrass productivity by $CO_2$ enrichment is expected based on $HCO_3^-$ use and the energetics of carbon uptake (Koch et al. 2013). Previous results from lab and mesocosm experiments are equivocal. Short-term measurements for some species indicate enhancement of photosynthesis by $CO_2$ enrichment, especially at high concentrations (Borum et al. 2016; Collier et al. 2018). Another study showed enhanced shoot production but not biomass-specific growth

(Palacios and Zimmerman 2007). Field studies that rely on gradients of $CO_2$ concentrations between different sites, for example, caused by proximity to a natural $CO_2$ vent have so far shown no consistent or pronounced response to elevated $CO_2$ concentrations (Ruesink et al. 2015; Takahashi et al. 2015; Koopmans et al. 2018). Our field study is not confounded by possible site variations and investigates how the same seagrass plant community responds to short-term, but substantial, natural diel oscillations in $CO_2$ and $O_2$ concentration levels. We find no evidence of $CO_2$ stimulation of photosynthesis under these dynamic conditions. Specifically, for both April and June, the lower and upper 25$^{th}$ percentiles of $pCO_2$:$O_2$ ratios (Fig. 8a,f), and the associated values of $pCO_2$ and $O_2$ concentrations behind the ratios (Fig. 8b,c,g,h), showed substantial and significant differences. Conversely, the PAR levels associated with the two percentiles (Fig. 8d,i) were not statistically different, allowing us to disregard effects of light. The analysis clearly shows that despite significant variations in $pCO_2$ and also in $O_2$ concentration under natural in situ conditions during the most productive spring and summer months, there was no stimulation of photosynthesis at high $pCO_2$ and low $O_2$ concentrations, nor limitation due to low $pCO_2$ and high $O_2$ concentrations, (Fig. 8e,j; $p = 0.64$ for April, $p = 0.53$ for June). Combining these results, we conclude that if seagrass photosynthetic production in our study was affected by naturally varying $CO_2$ concentrations, $O_2$ concentrations, or both, the effects were minor and could not be inferred from our in situ measurements.

**Summary**

Our work documents how dynamic whole-system seagrass metabolism can be on hourly, daily, and monthly time scales, and also, when combined with our previously published results for South Bay, on a yearly time scale. These dynamics included a trophic shift from autotrophy to heterotrophy from April to June. Faulty conclusions may be drawn if all the natural variations are not well integrated in seagrass metabolism measurements over the time interval for which one attempts to determine the trophic status.

Conversely, oscillating $O_2$ concentrations and $pCO_2$ in the water column were found to be driven mostly by the distinct day-night cycle in $O_2$ and $CO_2$ seagrass meadow production and consumption. Despite these variations in the water column that amounted to 4.5-fold for $pCO_2$ and 2.2-fold for $O_2$, we could not identify any effects on whole-system seagrass production. As a result, this field study does not support the notion that seagrass meadows may be "winners" in future oceans with elevated $CO_2$ concentrations. Conversely, we regrettably find it more likely that the accompanying elevated water temperatures will lead to more intense and more frequent harmful marine heatwave events that will negatively impact many temperate seagrass meadows.

There is a clear need for more studies on effects of temperature and other stressors on seagrasses, including changes in pH resulting from ocean acidification. These studies should include seagrasses in subtropical and tropical environments as well, and should, if at all possible, be done in situ to include the different time scales and natural drivers that influence and control seagrass metabolism.

## References


Alexandre, A., J. Silva, P. Buapet, M. Björk, and R. Santos. 2012. Effects of $CO_2$ enrichment on photosynthesis, growth, and nitrogen metabolism of the seagrass *Zostera noltii*. Ecol. Evol. **2**: 2625–2635. doi:10.1002/ece3.333

Arias-Ortiz, A., and others. 2018. A marine heatwave drives massive losses from the world's largest seagrass carbon stocks. Nat. Clim. Chang. **8**: 338–344. doi:10.1038/s41558-018-0096-y

Aufdenkampe, A. K., E. Mayorga, P. A. Raymond, J. M. Melack, S. C. Doney, S. R. Alin, R. E. Aalto, and K. Yoo. 2011. Riverine coupling of biogeochemical cycles between land, oceans, and atmosphere. Front. Ecol. Environ. **9**: 53–60. doi:10.1890/100014

Beck, M. W., and others. 2001. The identification, conservation, and management of estuarine and marine nurseries for fish and invertebrates: A better understanding of the habitats that serve as nurseries for marine species and the factors that create site-specific variability in nursery quality will improve conservation and management of these areas. AIBS Bull. **51**: 633–641.

Berg, P., H. Roy, F. Janssen, V. Meyer, B. B. Jorgensen, M. Huettel, and D. de Beer. 2003*a*. Oxygen uptake by aquatic sediments measured with a novel non-invasive eddy-correlation technique. Mar. Ecol. Prog. Ser. **261**: 75–83.

Berg, P., S. Rysgaard, and B. Thamdrup. 2003*b*. Dynamic modeling of early diagenesis and nutrient cycling. A case study in an Arctic marine sediment. Am. J. Sci. **303**: 905–955.

Berg, P., H. Roy, and P. L. Wiberg. 2007. Eddy correlation flux measurements: The sediment surface area that contributes to the flux. Limnol. Oceanogr. **52**: 1672–1684. doi:10.4319/lo.2007.52.4.1672

Berg, P., and M. Huettel. 2008. Monitoring the seafloor using the noninvasive eddy correlation technique: Integrated benthic exchange dynamics. Oceanography **21**: 164–167. doi:10.5670/oceanog.2008.13

Berg, P., R. N. Glud, A. Hume, H. Stahl, K. Oguri, V. Meyer, and H. Kitazato. 2009. Eddy correlation measurements of oxygen uptake in deep ocean sediments. Limnol. Oceanogr.: Methods **7**: 576–584. doi:10.4319/lom.2009.7.576

Berg, P., and others. 2013. Eddy correlation measurements of oxygen fluxes in permeable sediments exposed to varying current flow and light. Limnol. Oceanogr. **58**: 1329–1343. doi:10.4319/lo.2013.58.4.1329

Berg, P., C. E. Reimers, J. Rosman, M. Huettel, M. L. Delgard, and T. Özkan-Haller. 2015. Technical note: Time lag corrections of eddy correlation data measured in presence of waves. Biogeosci. **12**: 6721–6735. doi:10.5194/bgd-5112-8395-2015

Berg, P., M. L. Delgard, R. N. Glud, M. Huettel, C. E. Reimers, and M. L. Pace. 2017. Non-invasive flux measurements at the benthic interface: The aquatic eddy covariance technique. Limnol. Oceanogr.: E-Lectures. doi:10.1002/loe2.10005

Berner, R. A. 1980. Early diagenesis—a theoretical approach. Princeton Univ. Press.

Borges, A. V., B. Delille, L. S. Schiettecatte, F. Gazeau, G. Abril, and M. Frankignoulle. 2004. Gas transfer velocities of $CO_2$ in three European estuaries (Randers Fjord, Scheldt, and Thames). Limnol. Oceanogr. **49**: 1630–1641. doi:10.4319/lo.2004.49.5.1630

Borum, J., K. Sand-Jensen, T. Binzer, O. Pedersen, and T. M. Greve. 2007. Oxygen movement in seagrasses, p. 255–270. *In* A. W. Larkum, R. J. Orth, and C. Duarte [eds.], Seagrasses: Biology, ecology and conservation. Springer.

Borum, J., O. Pedersen, L. Kotula, M. W. Fraser, J. Statton, T. D. Colmer, and G. A. Kendrick. 2016. Photosynthetic response to globally increasing $CO_2$ of CO-occurring temperate seagrass species. Plant Cell Environ. **39**: 1240–1250. doi:10.1111/pce.12658

Boudreau, B. 1997. Diagenetic models and their implementation: Modelling transport and reactions in aquatic sediments. Springer.

Bouillon, S., J. J. Middelburg, F. Dehairs, A. V. Borges, G. Abril, M. R. Flindt, S. Ulomi, and E. Kristensen. 2007. Importance of intertidal sediment processes and porewater exchange on the water column biogeochemistry in a pristine mangrove creek (Ras Dege, Tanzania). Biogeosciences **4**: 311–322. doi:10.5194/bg-4-311-2007

Buapet, P., L. M. Rasmusson, M. Gullström, and M. Björk. 2013. Photorespiration and carbon limitation determine productivity in temperate seagrasses. PLoS One **8**: e83804. doi:10.1371/journal.pone.0083804

Cai, W. J., X. Hu, W. J. Huang, L. Q. Jiang, Y. Wang, T. H. Peng, and X. Zhang. 2010. Alkalinity distribution in the western North Atlantic Ocean margins. J. Geophys. Res. Oceans **115**: C08014. doi:10.1029/2009JC005482

Canfield, D. E., and others. 1993. Pathways of organic carbon oxidation in three continental margin sediments. Mar. Geol. **113**: 27–40. doi:10.1016/0025-3227(93)90147-N

Carr, J. A., P. D'Odorico, K. J. McGlathery, and P. L. Wiberg. 2016. Spatially explicit feedbacks between seagrass meadow structure, sediment and light: Habitat suitability for seagrass growth. Adv. Water Resour. **93**: 315–325. doi:10.1016/j.advwatres.2015.09.001

Challener, R. C., L. L. Robbins, and J. B. McClintock. 2016. Variability of the carbonate chemistry in a shallow, seagrass-dominated ecosystem: Implications for ocean acidification experiments. Mar. Freshw. Res. **67**: 163–172. doi:10.1071/MF14219

Collier, C. J., L. Langlois, Y. Ow, C. Johansson, M. Giammusso, M. P. Adams, K. R. O'Brien, and S. Uthicke. 2018. Losing a winner: Thermal stress and local pressures outweigh the positive effects of ocean acidification for tropical seagrasses. New Phytol. **219**: 1005–1017. doi:10.1111/nph.15234

Costanza, R., and others. 1997. The value of the world's ecosystem services and natural capital. Nature **387**: 253–260. doi:10.1038/387253a0

Dai, M., Z. Lu, W. Zhai, B. Chen, Z. Cao, K. Zhou, W. J. Cai, and C. T. A. Chenc. 2009. Diurnal variations of surface seawater $pCO_2$ in contrasting coastal environments. Limnol. Oceanogr. **54**: 735–745. doi:10.4319/lo.2009.54.3.0735

Dickson, A., and F. Millero. 1987. A comparison of the equilibrium constants for the dissociation of carbonic acid in seawater media. Deep-Sea Res. Part A Oceanogr. Res. Pap. **34**: 1733–1743. doi:10.1016/0198-0149(87)90021-5

Duarte, C. M., J. J. Middelburg, and N. Caraco. 2005. Major role of marine vegetation on the oceanic carbon cycle. Biogeosciences **2**: 1–8. doi:10.5194/bg-2-1-2005

Duarte, C. M., N. Marbà, E. Gacia, J. W. Fourqurean, J. Beggins, C. Barrón, and E. T. Apostolaki. 2010. Seagrass community metabolism: Assessing the carbon sink capacity of seagrass meadows. Global Biogeochem. Cycles **24**. GB4032. doi:10.1029/2010GB003793

Duarte, C. M., and others. 2013*a*. Is ocean acidification an open-ocean syndrome? Understanding anthropogenic impacts on seawater pH. Estuaries Coast. **36**: 221–236.

Duarte, C. M., I. J. Losada, I. E. Hendriks, I. Mazarrasa, and N. Marbà. 2013*b*. The role of coastal plant communities for climate change mitigation and adaptation. Nat. Clim. Chang. **3**: 961–968.

Fan, S. M., S. C. Wofsy, P. S. Bakwin, D. J. Jacob, and D. R. Fitzjarrald. 1990. Atmosphere-biosphere exchange of $CO_2$ and $O_3$ in the central Amazon Forest. J. Geophys. Res. Atmos. **95**: 16851–16864. doi:10.1029/JD095iD10p16851

Feely, R. A., C. L. Sabine, J. M. Hernandez-Ayon, D. Ianson, and B. Hales. 2008. Evidence for upwelling of corrosive "acidified" water onto the continental shelf. Science **320**: 1490–1492. doi:10.1126/science.1155676

Ge, X., Y. Kostov, R. Henderson, N. Selock, and G. Rao. 2014. A low-cost fluorescent sensor for $pCO_2$ measurements. Chemosensors **2**: 108–120.

Glud, R. N. 2008. Oxygen dynamics of marine sediments. Mar. Biol. Res. **4**: 243–289. doi:10.1080/17451000801888726

Greiner, J. T., K. J. McGlathery, J. Gunnell, and B. A. McKee. 2013. Seagrass restoration enhances "blue carbon" sequestration in coastal waters. PLoS One **8**: e72469. doi:10.1371/journal.pone.0072469

Greve, T. M., J. Borum, and O. Pedersen. 2003. Meristematic oxygen variability in eelgrass (*Zostera marina*). Limnol. Oceanogr. **48**: 210–216. doi:10.4319/lo.2003.48.1.0210

Greve, T. M., D. Krause-Jensen, M. B. Rasmussen, and P. B. Christensen. 2005. Means of rapid eelgrass (*Zostera marina* L.) recolonisation in former dieback areas. Aquat. Bot. **82**: 143–156. doi:10.1016/j.aquabot.2005.03.004

Guo, H., A. Noormets, B. Zhao, J. Chen, G. Sun, Y. Gu, B. Li, and J. Chen. 2009. Tidal effects on net ecosystem exchange of carbon in an estuarine wetland. Agric. For. Meteorol. **149**: 1820–1828. doi:10.1016/j.agrformet.2009.06.010

Hammer, K. J., J. Borum, H. Hasler-Sheetal, E. C. Shields, K. Sand-Jensen, and K. A. Moore. 2018. High temperatures cause reduced growth, plant death and metabolic changes in eelgrass *Zostera marina*. Mar. Ecol. Prog. Ser. **604**: 121–132. doi:10.3354/meps12740

Hansen, J. C., and M. A. Reidenbach. 2012. Wave and tidally driven flows in eelgrass beds and their effect on sediment suspension. Mar. Ecol. Prog. Ser. **448**: 271–287. doi:10.3354/meps09225

Hejnowicz, A. P., H. Kennedy, M. A. Rudd, and M. R. Huxham. 2015. Harnessing the climate mitigation, conservation and poverty alleviation potential of seagrasses: Prospects for developing blue carbon initiatives and payment for ecosystem service programmes. Front. Mar. Sci. **2**: 32.

Hendriks, I. E., Y. Olsen, L. Ramajo, L. Basso, A. Steckbauer, T. Moore, J. Howard, and C. Duarte. 2014. Photosynthetic activity buffers ocean acidification in seagrass meadows. Biogeosciences **11**: 333–346. doi:10.5194/bg-11-333-2014

Howard, J. L., J. C. Creed, M. V. Aguiar, and J. W. Fouqurean. 2018. $CO_2$ released by carbonate sediment production in some coastal areas may offset the benefits of seagrass "blue carbon" storage. Limnol. Oceanogr. **63**: 160–172. doi:10.1002/lno.10621

Hume, A. C., P. Berg, and K. J. McGlathery. 2011. Dissolved oxygen fluxes and ecosystem metabolism in an eelgrass (*Zostera marina*) meadow measured with the eddy correlation technique. Limnol. Oceanogr. **56**: 86–96. doi:10.4319/lo.2011.56.1.0086

Jassby, A. D., and T. Platt. 1976. Mathematical formulation of relationship between photosynthesis and light for phytoplankton. Limnol. Oceanogr. **21**: 540–547. doi:10.4319/lo.1976.21.4.0540

Johannessen, S. C., and R. W. Macdonald. 2016. Geoengineering with seagrasses: Is credit due where credit is given? Environ. Res. Lett. **11**: 113001. doi:10.1088/1748-9326/11/11/113001

Koch, M., G. Bowes, C. Ross, and X. H. Zhang. 2013. Climate change and ocean acidification effects on seagrasses and marine macroalgae. Glob. Chang. Biol. **19**: 103–132. doi:10.1111/j.1365-2486.2012.02791.x

Koopmans, D., M. Holtappels, A. Chennu, M. Weber, and D. de Beer. 2018. The response of seagrass (*Posidonia oceanica*) meadow metabolism to $CO_2$ levels and hydrodynamic exchange determined with aquatic eddy covariance. Biogeosci. Discuss. doi:10.5194/bg-2018-5199

Lee, X., W. Massman, and B. Law. 2004. Handbook of micrometeorology: A guide for surface flux measurement and analysis. Kluwer Academic Publishers.

Lewis, E., D. Wallace, and L. J. Allison. 1998. Program developed for $CO_2$ system calculations. Dept. of Applied Science, Brookhaven National Lab.; Oak Ridge National Lab., Carbon Dioxide Information Analysis Center.

Long, M. H., J. E. Rheuban, P. Berg, and J. C. Zieman. 2012. A comparison and correction of light intensity loggers to photosynthetically active radiation sensors. Limnol. Oceanogr.: Methods, **10**: 416–424. doi:10.4319/lom.2012.10.416

Lorrai, C., D. F. McGinnis, P. Berg, A. Brand, and A. Wüest. 2010. Application of oxygen eddy correlation in aquatic systems. J. Atmos. Ocean. Technol. **27**: 1533–1546. doi:10.1175/2010JTECHO723.1

Macreadie, P. I., O. Serrano, D. T. Maher, C. M. Duarte, and J. Beardall. 2017. Addressing calcium carbonate cycling in blue carbon accounting. Limnol. Oceanogr.: Lett. **2**: 195–201. doi:10.1002/lol2.10052

Macreadie, P. I., C. J. Ewers-Lewis, A. A. Whitt, Q. Ollivier, S. M. Trevathan-Tackett, P. Carnell, and O. Serrano. 2018. Comment on 'Geoengineering with seagrasses: Is credit due where credit is given?'. Environ. Res. Lett. **13**: 028002. doi:10.1088/1748-9326/aaa7ad.

Marba, N., and C. M. Duarte. 2010. Mediterranean warming triggers seagrass (*Posidonia oceanica*) shoot mortality. Glob. Chang. Biol. **16**: 2366–2375.

Mass, T., A. Genin, U. Shavit, M. Grinstein, and D. Tchernov. 2010. Flow enhances photosynthesis in marine benthic autotrophs by increasing the efflux of oxygen from the organism to the water. Proc. Natl. Acad. Sci. USA **107**: 2527–2531.

Mazarrasa, I., and others. 2015. Seagrass meadows as a globally significant carbonate reservoir. Biogeosciences. **12**: 4993–5003. doi:10.5194/bg-12-4993-2015.

McGinnis, D. F., P. Berg, A. Brand, C. Lorrai, T. J. Edmonds, and A. Wüest. 2008. Measurements of eddy correlation oxygen fluxes in shallow freshwaters: Towards routine applications and analysis. Geophys. Res. Lett. **35**: L04403.

McGinnis, D. F., S. Cherednichenko, S. Sommer, P. Berg, L. Rovelli, R. Schwarz, R. N. Glud, and P. Linke. 2011. Simple, robust eddy correlation amplifier for aquatic dissolved oxygen and hydrogen sulfide flux measurements. Limnol. Oceanogr.: Methods **9**: 340–347. doi:10.4319/lom.2011.9.340

McGlathery, K. J., K. Sundbäck, and I. C. Anderson. 2007. Eutrophication in shallow coastal bays and lagoons: The role of plants in the coastal filter. Mar. Ecol. Prog. Ser. **348**: 1–18. doi:10.3354/meps07132

McGlathery, K. J., L. K. Reynolds, L. W. Cole, R. J. Orth, S. R. Marion, and A. Schwarzschild. 2012. Recovery trajectories during state change from bare sediment to eelgrass dominance. Mar. Ecol. Prog. Ser. **448**: 209–221. doi:10.3354/meps09574

Mcleod, E., and others. 2011. A blueprint for blue carbon: Toward an improved understanding of the role of vegetated coastal habitats in sequestering $CO_2$. Front. Ecol. Environ. **9**: 552–560. doi:10.1890/110004

Moore, K. A., and J. C. Jarvis. 2008. Environmental factors affecting recent summertime eelgrass diebacks in the lower Chesapeake Bay: Implications for long-term persistence. J. Coast. Res. **55**: 135–147. doi:10.2112/SI55-014

Moore, K. A., E. C. Shields, D. B. Parrish, and R. J. Orth. 2012. Eelgrass survival in two contrasting systems: Role of turbidity

and summer water temperatures. Mar. Ecol. Prog. Ser. **448**: 247–258. doi:10.3354/meps09578

Murray, B. C., L. Pendleton, W. A. Jenkins, and S. Sifleet. 2011. Green payments for blue carbon: Economic incentives for protecting threatened coastal habitats. Report NI 11. Nicholas Institute for Environmental Policy Solutions.

Oreska, M. P., K. J. McGlathery, and J. H. Porter. 2017. Seagrass blue carbon spatial patterns at the meadow-scale. PLoS One **12**: e0176630. doi:10.1371/journal.pone.0176630

Oreska, M. P., K. J. McGlathery, I. M. Emmer, B. A. Needelman, S. Emmett-Mattox, S. Crooks, J. P. Megonigal, and D. Myers. 2018. Comment on 'Geoengineering with seagrasses: Is credit due where credit is given?'. Environ. Res. Lett. **13**: 038001. doi:10.1088/1748-9326/aaae72

Orr, J., J.-M. Epitalon, and J.-P. Gattuso. 2015. Comparison of ten packages that compute ocean carbonate chemistry. Biogeosci. **12**: 1483–1510. doi:10.5194/bg-12-1483-2015

Orth, R. J., M. L. Luckenbach, S. R. Marion, K. A. Moore, and D. J. Wilcox. 2006. Seagrass recovery in the Delmarva Coastal Bays, USA. Aquat. Bot. **84**: 26–36. doi:10.1016/j.aquabot.2005.07.007

Orth, R. J., S. R. Marion, K. A. Moore, and D. J. Wilcox. 2010. Eelgrass (*Zostera marina* L.) in the Chesapeake Bay region of mid-Atlantic coast of the USA: Challenges in conservation and restoration. Estuaries Coast. **33**: 139–150.

Orth, R. J., and K. J. McGlathery. 2012. Eelgrass recovery in the coastal bays of the Virginia Coast Reserve, USA. Mar. Ecol. Prog. Ser. **448**: 173–176. doi:10.3354/meps09596

Pacella, S. R., C. A. Brown, G. G. Waldbusser, R. G. Labiosa, and B. Hales. 2018. Seagrass habitat metabolism increases short-term extremes and long-term offset of $CO_2$ under future ocean acidification. Proc. Natl. Acad. Sci. USA **115**: 3870–3875. doi:10.1073/pnas.1703445115

Palacios, S. L., and R. C. Zimmerman. 2007. Response of eelgrass *Zostera marina* to $CO_2$ enrichment: Possible impacts of climate change and potential for remediation of coastal habitats. Mar. Ecol. Prog. Ser. **344**: 1–13.

Pedersen, O., T. D. Colmer, and K. Sand-Jensen. 2013. Underwater photosynthesis of submerged plants–recent advances and methods. Front. Plant Sci. **4**: 140. doi:10.3389/fpls.2013.00140

Pedersen, O., T. D. Colmer, J. Borum, A. Zavala-Perez, and G. A. Kendrick. 2016. Heat stress of two tropical seagrass species during low tides–impact on underwater net photosynthesis, dark respiration and diel in situ internal aeration. New Phytol. **210**: 1207–1218. doi:10.1111/nph.13900

Raven, J., and A. Larkum. 2007. Are there ecological implications for the proposed energetic restrictions on photosynthetic oxygen evolution at high oxygen concentrations? Photosynth. Res. **94**: 31–42. doi:10.1007/s11120-007-9211-z

Raymond, P., and J. Cole. 2001. Gas exchange in rivers and estuaries: Choosing a gas transfer velocity. Estuaries **24**: 312–317. doi:10.2307/1352954

Reimers, C. E., T. Özkan-Haller, P. Berg, A. Devol, K. McCann-Grosvenor, and R. D. Sanders. 2012. Benthic oxygen consumption rates during hypoxic conditions on the Oregon continental shelf: Evaluation of the eddy correlation method. J. Geophys. Res. **117**: 1–18.

Reynolds, L. K., M. Waycott, and K. J. McGlathery. 2013. Restoration recovers population structure and landscape genetic connectivity in a dispersal-limited ecosystem. J. Ecol. **101**: 1288–1297.

Rheuban, J. E. 2013. Oxygen metabolism in restored eelgrass (*Zostera marina* L.) meadows measured by eddy correlation. Master of Science thesis. Univ. of Virginia.

Rheuban, J. E., and P. Berg. 2013. The effects of spatial and temporal variability at the sediment surface on aquatic eddy correlation flux measurements. Limnol. Oceanogr.: Methods **11**: 351–359.

Rheuban, J. E., P. Berg, and K. J. McGlathery. 2014*a*. Ecosystem metabolism along a colonization gradient of eelgrass (*Zostera marina*) measured by eddy correlation. Limnol. Oceanogr. **59**: 1376–1387.

Rheuban, J. E., P. Berg, and K. J. McGlathery. 2014*b*. Multiple timescale processes drive ecosystem metabolism in eelgrass (*Zostera marina*) meadows. Mar. Ecol. Prog. Ser. **507**: 1–13.

Ruesink, J. L., S. Yang, and A. C. Trimble. 2015. Variability in carbon availability and eelgrass (*Zostera marina*) biometrics along an estuarine gradient in Willapa Bay, WA, USA. Estuaries Coast. **38**: 1908–1917. doi:10.1007/s12237-014-9933-z

Saderne, V., P. Fietzek, and P. M. J. Herman. 2013. Extreme variations of $pCO_2$ and pH in a macrophyte meadow of the Baltic Sea in summer: Evidence of the effect of photosynthesis and local upwelling. PLoS One **8**: e62689. doi:10.1371/journal.pone.0062689

Saderne, V., and others. 2019. Role of carbonate burial in Blue Carbon budgets. Nat. Commun. **10**: 1106.

Schar, D. W., M. J. Atkinson, T. H. Johengen, A. Pinchuk, H. Purcell, C. Y. Robertson, G. J. Smith, and M. N. Tamburri. 2010. Performance demonstration statement for Pro-Oceanus Systems Inc. PSI CO2-pro. Alliance for Coastal Technologies (ACT).

Semesi, I. S., S. Beer, and M. Björk. 2009. Seagrass photosynthesis controls rates of calcification and photosynthesis of calcareous macroalgae in a tropical seagrass meadow. Mar. Ecol. Prog. Ser. **382**: 41–47. doi:10.3354/meps07973

Staehr, P. A., and J. Borum. 2011. Seasonal acclimation in metabolism reduces light requirements of eelgrass (*Zostera marina*). J. Exp. Mar. Biol. Ecol. **407**: 139–146. doi:10.1016/j.jembe.2011.05.031

Stocker, T. 2014. Climate change 2013: The physical science basis: Working group I contribution to the fifth assessment report of the Intergovernmental Panel on Climate Change. Cambridge Univ. Press.

Takahashi, M., S. Noonan, K. Fabricius, and C. Collier. 2015. The effects of long-term in situ $CO_2$ enrichment on tropical seagrass communities at volcanic vents. ICES J. Mar. Sci. **73**: 876–886.

Takahashi, T., and others. 2002. Global sea–air $CO_2$ flux based on climatological surface ocean $pCO_2$, and seasonal biological and temperature effects. Deep-Sea Res. Part II Top. Stud. Oceanogr. **49**: 1601–1622. doi:10.1016/S0967-0645(02)00003-6

Thomson, J. A., D. A. Burkholder, M. R. Heithaus, J. W. Fourqurean, M. W. Fraser, J. Statton, and G. A. Kendrick. 2015. Extreme temperatures, foundation species, and abrupt ecosystem change: An example from an iconic seagrass ecosystem. Glob. Chang. Biol. **21**: 1463–1474. doi:10.1111/gcb.12694

Van Cappellen, P., and Y. F. Wang. 1996. Cycling of iron and manganese in surface sediments: A general theory for the coupled transport and reaction of carbon, oxygen, nitrogen, sulfur, iron, and manganese. Am. J. Sci. **296**: 197–243. doi:10.2475/ajs.296.3.197

Van Heuven, S., D. Pierrot, J. Rae, E. Lewis, and D. Wallace. 2011. MATLAB program developed for $CO_2$ system calculations. ORNL/CDIAC-105b. Carbon Dioxide Information Analysis Center, Oak Ridge National Laboratory, US Department of Energy.

Waldbusser, G. G., and J. E. Salisbury. 2014. Ocean acidification in the coastal zone from an organism's perspective: Multiple system parameters, frequency domains, and habitats. Ann. Rev. Mar. Sci. **6**: 221–247. doi:10.1146/annurev-marine-121211-172238

Wang, Z. A., and W. J. Cai. 2004. Carbon dioxide degassing and inorganic carbon export from a marsh-dominated estuary (the Duplin River): A marsh $CO_2$ pump. Limnol. Oceanogr. **49**: 341–354. doi:10.4319/lo.2004.49.2.0341

Wanninkhof, R., D. Bakker, N. Bates, A. Olsen, T. Steinhoff, and A. Sutton. 2013. Incorporation of alternative sensors in the SOCAT database and adjustments to dataset quality control flags. Carbon Dioxide Information Analysis Center, Oak Ridge National Laboratory, US Department of Energy.

Wiberg, P. L., J. A. Carr, I. Safak, and A. Anutaliya. 2015. Quantifying the distribution and influence of non-uniform bed properties in shallow coastal bays. Limnol. Oceanogr.: Methods **13**: 746–762.

Yates, K. K., C. Dufore, N. Smiley, C. Jackson, and R. B. Halley. 2007. Diurnal variation of oxygen and carbonate system parameters in Tampa Bay and Florida Bay. Mar. Chem. **104**: 110–124. doi:10.1016/j.marchem.2006.12.008

Zhai, W., Y. Ko, W. Zhu, A. Wong, and C. B. Park. 2009. A study of the crystallization, melting, and foaming behaviors of polylactic acid in compressed $CO_2$. Int. J. Mol. Sci. **10**: 5381–5397. doi:10.3390/ijms10125381

Zimmerman, R. C., D. G. Kohrs, D. L. Steller, and R. S. Alberte. 1997. Impacts of $CO_2$ enrichment on productivity and light requirements of eelgrass. Plant Physiol. **115**: 599–607. doi:10.1104/pp.115.2.599

## Acknowledgments

We thank Chris Buck, David Boyd, Lillian Aoki, and Art Schwarzschild for their help collecting data. Support for this study was provided by the University of Virginia, the National Science Foundation through grants to Peter Berg from Chemical Oceanography (OCE-1061364) and Ocean Technology and Interdisciplinary Coordination (OCE-1334848), from the Division of Environmental Biology to the Virginia Coast Reserve Long Term Ecological Research Program (DEB-1237733 and DEB-1832221), and the French Research Institute for Exploitation of the Sea (IFREMER).

## Conflict of Interest

None declared.

*Submitted 12 February 2019*
*Revised 13 May 2019*
*Accepted 16 May 2019*

*Associate editor: Ronnie Glud*